**Thesis for the Degree of Doctor of Philosophy**

# Physically Crosslinked and Chemically Photocrosslinked Silk Hydrogel Manipulated via Molecular Weight Control

분자량조절기법을 이용하여 제조한 물리적 가교 및 화학적 광가교 실크 하이드로젤

**February 2017**

**By**

**Kim, Hyung Hwan**

**Department of Biosystems & Biomaterials**

**Science and Engineering**

**SEOUL NATIONAL UNIVERSITY**

**Thesis for the Degree of Doctor of Philosophy**

# Physically Crosslinked and Chemically Photocrosslinked Silk Hydrogel Manipulated via Molecular Weight Control

**February 2017**

**By**

**Kim, Hyung Hwan**

**Department of Biosystems & Biomaterials**

**Science and Engineering**

**SEOUL NATIONAL UNIVERSITY**

**Thesis for the Degree of Doctor of Philosophy**

# Physically Crosslinked and Chemically Photocrosslinked Silk Hydrogel Manipulated via Molecular Weight Control

**A Thesis Submitted to the Faculty of Seoul National University**

**in Partial Fulfillment of the Requirements for**

**the Degree of Doctor of Philosophy**

**By**

**Kim, Hyung Hwan**

**Advisor : Professor Young Hwan Park, Ph.D.**

**February 2017**

**Department of Biosystems & Biomaterials**

**Science and Engineering**

**SEOUL NATIONAL UNIVERSITY**

**Department of Biosystems & Biomaterials**

**Science and Engineering**

**SEOUL NATIONAL UNIVERSITY**

**Supervisory Committee Approval**

**of Thesis submitted by**

**Kim, Hyung Hwan**

**This thesis has been read by each member of the following supervisory committee and has been found to be satisfactory.**

**Chairman of Committee :**

_____

**Hyun, Jin Ho**

**Vice Chairman of Committee :**

_____

**Park, Young Hwan**

**Member of Committee :**

_____

**Lee, Ki Hoon**

**Member of Committee :**

_____

**Lee, Han Sup**

**Member of Committee :**

_____

**Um, In Chul**

# Physically Crosslinked and Chemically Photocrosslinked Silk Hydrogel Manipulated via Molecular Weight Control

## 분자량조절기법을 이용하여 제조한 물리적 가교 및 화학적 광가교 실크 하이드로젤

지도교수 박 영 환

이 논문을 박사 학위논문으로 제출함

2016년 11월

서울대학교 대학원
바이오시스템·소재학부
바이오소재전공
김 형 환

김형환의 박사 학위논문을 인준함

2017년 1월

위 원 장 현 진 호 (인)

부위원장 박 영 환 (인)

위 원 이 기 훈 (인)

위 원 이 한 섭 (인)

위 원 엄 인 철 (인)

# Abstract

In this study, alkaline hydrolysis was utilized using heat-alkaline treatment (HAT) method to manipulate the silk hydrogel properties. By regulating the hydrolysis time (10-180 min), a broad molecular weight range of silk fibroin (SF) could be obtained (77.2-258.6 kDa). The change of molecular weight of SF also greatly affected the physical properties (i.e., swelling ratio, shear modulus, transparency) of SF hydrogel. As a result of structural analysis, the molecular weight of SF played a crucial role in the construction of microstructure of SF hydrogel. These findings indicate that physically crosslinked SF hydrogels of variable physical properties can be fabricated based on molecular weight control. However, this manipulation could not improve the mechanical property (i.e., brittleness) of typical SF hydrogel in addition to a long gelation time. Chemical crosslinking of SF can overcome these problems by making strong covalent bond in a network within predictable gelation time. Therefore, new strategy was developed for making chemically photo-crosslinked SF hydrogel without using of fresh SF aqueous solution. By lowering the molecular weight of SF, the stability of SF aqueous solution could be enhanced and consequently, this allowed direct chemical modification of SF. Subsequently, photo-crosslinkable silk fibroin methacrylate (SFMA) was synthesized using the hydrolyzed SF and chemically photo-crosslinked SF hydrogel (SFMA hydrogel) could be fabricated with a rapid gel formation. The structural characteristics, physical properties, and performance of chemically crosslinked SF hydrogel were intensively examined on the effect of immobilized MA amount on SF and molecular weight of SF. It is expected that SFMA hydrogel has a high

potential use in biomedical applications due to its excellent gel properties and performance (e.g., transparency, resiliency, and injectability).

---

**Keywords:** Silk fibroin, Methacrylate, Hydrogel, Alkaline hydrolysis, Physical crosslinking, Chemical crosslinking, Photo-crosslinking

**Student number: 2011-21249**

# CONTENTS

# List of Tables

# List of Figures

# I. INTRODUCTION

Silk fibroin (SF) is a major protein, which plays a critical role in both structural feature and mechanical property of silk cocoons. To date, it has been widely reported that SF can be used in biomedical applications due to excellent biocompatibility and superior mechanical property [1-6]. Besides, the facile recrystallization by alcohol treatment, inducing the physical crosslinking via intra- and inter-molecular hydrogen bonding of hydrophobic segments of SF, is generally exploited in the fabrication process for SF [7, 8]. Such a process is very useful in biomedical application fields (e.g., tissue engineering scaffold, drug carrier, etc.) since this process does not cause any harmful damaging to living organisms.

SF can be easily fabricated into various forms (e.g., film, nanofiber, sponge, hydrogel, etc.) [9]. Among various types and shapes of SF, numerous trials were progressed to develop the SF hydrogel for biomedical applications. It is because highly porous network structure of hydrogel retains a large amount of water with inter-connected porous structure, which can facilitate the encapsulation of inorganic particles, drugs, and even the living cells [6]. Moreover, structural feature of the hydrogel provides physiologically stable condition for cell survival with appropriate three-dimensional (3D) microenvironment that allows the cell survival with growth *in vitro* and *in vivo* [10-12]. Therefore, SF hydrogel can exhibit excellent biological behavior and superior to synthetic polymer-based hydrogel (e.g., poly(ethylene glycol)

[13], poly(vinyl alcohol) [14]) as a 3D cell niche.

Another interesting structural feature of SF, compared to other polymeric materials, is that unique structural transition occurs during hydrogel network formation. It is known that major protein of SF chains in crystalline region is consisted of repeated glycine (G) -alanine (A) segment (GAGAGX, X = Ser or Tyr) that can build the insoluble anti-parallel β-sheet structure [15]. Meanwhile, in aqueous solution state, SF chains exist as a random-coil conformation [16]. However, it is thermodynamically unstable to maintain this structural conformation in aqueous solution. As a consequence, structural transition occurs to β-sheet conformation by accompanying with chain aggregation [17, 18]. On a macroscopic level, the SF chains finally construct physically crosslinked network structure of hydrogel via hydrogen bonding formation.

Due to its structural difference, properties of SF hydrogel are affected by a wide variety of processing parameters, such as concentration of SF solution [19, 20], incubation temperature [19], vortexing time [21], and ultra-sonic power [22]. The concentration is a major factor to determine physical properties of SF hydrogel. Generally, higher concentration results in stiffer hydrogels with a shorter gelation time. The gelation behavior is also largely dependent on the incubation temperature [19]. For example, the SF hydrogel formed at a higher temperature (~50°C) mostly has a higher Young's modulus than that formed at a lower temperature (~4°C). The effect of amplitude of

shear force was also investigated. X. Wang *et al*. showed that the amplitude of ultra-sonication affected the mechanical properties of SF hydrogel [22]. T. Yucel *et al*. reported the effect of vortexing time on the shear modulus of SF hydrogel [21]. Although many studies for manipulating SF hydrogel properties were reported, none of processing variables could elicit the change of a wide range in mechanical as well as physical properties except the concentration of the precursor SF solution.

Generally, the molecular weight of polymer composing network structure of hydrogel is a crucial factor that determines the gel properties (i.e., modulus, swelling ratio, permeability) [23-25]. Both crosslinking density and mesh size of hydrogel are largely dependent on the polymer chain length regardless of crosslinking methods (i.e., chemical or physical crosslinking) [26, 27]. Nevertheless, the effect of molecular weight of SF on hydrogel fabrication has not been explored. Hence, in this study, the heat-alkaline treatment (HAT) was conducted during SF dissolution step to control the molecular weight of SF as a one-pot process. This method is not only simple but also suitable to obtain a high yield of hydrolyzed SF. In contrast, proteinase treatment needs relatively delicate process including enzyme removing process and causes severe mass loss of product in spite of high efficiency [28].

After the HAT, hydrolyzed SF was used for the fabrication of hydrogel using ultra-sonication method. Then, physical and mechanical property analyses were performed in order to investigate the effect of molecular weight of SF on

the hydrogel formation. By controlling the molecular weight of SF, it was possible to manipulate the structure, performance and physical properties of physically crosslinked SF hydrogel in a wide range for their proper applications.

Nevertheless, poor mechanical property of typical SF hydrogel, which being vulnerable to shear deformation (e.g., bending, twisting, etc.), was pointed out as a limitation of real applications in tissue engineering. It is because hydrogen bonding formed in physical crosslinking is inherently weak against shear deformation. Also, crystallinity of physically crosslinked SF hydrogel is too low even though β-sheet crystalline structure formed. Regenerated SF generally shows a lower degree of crystallinity compared to natural SF fibers [29]. In case of regenerated SF film, it becomes brittle after insolubilization and crystallization treatment, in which SF chains are transformed into β-sheet crystalline conformation. Most of regenerated SF forms exhibit poor mechanical behavior unless chemical treatment is carried out.

To enhance the mechanical property of SF hydrogel, introduction of chemical crosslinking might be an alternative strategy for its better performance. Many chemical crosslinkers were investigated for the linkage of hydroxyl or amine groups in SF [30-34]. Enzymes (e.g., horseradish peroxidase [35], tyrosinase [36], etc.) can also be utilized for chemical crosslinking of SF in aqueous solution state via di-tyrosine linkage formation. This enzyme treatment is considerably biocompatible compared to usage of

chemical crosslinkers. Recently, M.B. Applegate *et al*. reported that photo-initiator, riboflavin, could be used for photo-crosslinking of SF hydrogel via inter-covalent bond formation between tyrosine groups in SF and this SF hydrogel showed high resilience property [37]. However, chemical crosslinking strategies still have some limitations in an application of SF hydrogel because fresh SF aqueous solution is required for hydrogel fabrication. Substantially, SF aqueous solution is difficult to manipulate and hard to maintain its pure state due to innate instability.

Here, a new fabrication method was developed for making chemically photo-crosslinked SF hydrogel with excellent physical properties and high performance. First, the alkaline hydrolysis was conducted to manipulate a molecular weight of SF, which can make enhancing a stability of SF in aqueous solution. Consequently, this strategy is feasible for the application as ready-to-use SF hydrogel without an instant preparation of fresh SF aqueous solution. In addition, this allowed direct chemical modification of SF without any precipitation during chemical reaction and dialysis process. It has been reported that due to the instability of SF, it was hard to modify the SF chemically in aqueous solution state except hydrophilic silk sericin [38].

In this study, photo-crosslinking method was utilized by introducing methacrylate (MA) groups onto SF, with a use of photo-initiator. Using the hydrolyzed SF, MA-immobilized SF (silk fibroin methacrylate, SFMA) was synthesized and photo-crosslinkable SF hydrogel was then fabricated. The

structure, physical properties, and performance of the chemically photo-crosslinked SF hydrogel (SFMA hydrogel) were evaluated on the effect of immobilized MA amount on SF.

Therefore, in the first part, the physically crosslinked SF hydrogels with various molecular weights of SF were fabricated and the effect of its molecular weight on microstructure and hydrogel properties was investigated using a novel hydrolysis technique (HAT method). For the second part, the chemically photo-crosslinked SF hydrogel was fabricated using the hydrolyzed (molecular weight controlled) SFMA and evaluated its microstructure and properties. In order to find out its excellent physical property and performance, gelation behavior, gel property, transparency, thixotropic property, resilience, and degradation behavior of the photo-crosslinked SF hydrogel were intensively studied for determining its feasible use in biomedical applications.

# II. LITERATURE SURVEY

## 2.1. SILK FIBROIN (SF) AS A BIOMATERIAL

Silk fibroin (SF) is a major fibrous protein, which plays a critical role in both structural feature and mechanical property of silk cocoons, which are produced by silkworms (*Bombyx mori*). In raw silk fibers, two SF strands are covered with a gum-like adhesive protein, known as silk sericin (SS) (**Figure 1**) [39], which occupies 25-30 wt% of total silkworm cocoon. The SF consists of a heavy chain ($M_w$ ~ 390 kDa) and a light chain ($M_w$ ~ 25 kDa) linked by a disulfide bond [9, 40]. In silkworm gland, the SF exists as a sol state with a random coil conformation. During spinning process of fiber formation, the SF becomes concentrated, pH of the solution is changed to acidic condition, and shear stress is applied [41, 42]. These environmental changes tend to occur the structural transition of hydrophobic repeating unit of SF (Gly-Ala-Gly-Ala-Gly-X, X = Ser or Tyr) into a crystalline solid state with insolubilization. The β-sheet conformation of macromolecular chains is a well-known secondary structure of SF fiber. When silk fiber is spun from the silkworm spinneret with stretching, the β-sheet crystal domains are highly aligned to longitudinal direction of fiber axis. Consequently, raw silk fiber shows excellent tensile property due to its highly oriented crystalline structure. Ultimate tensile strength of *B.mori* silk fibers is 740 MPa. While, collagen and poly (lactic acid) (PLA) has ultimate tensile strength of 0.9-7.4 MPa and 28-50 MPa, respectively [43].

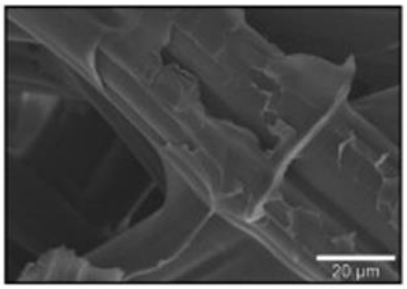


electron micrograph

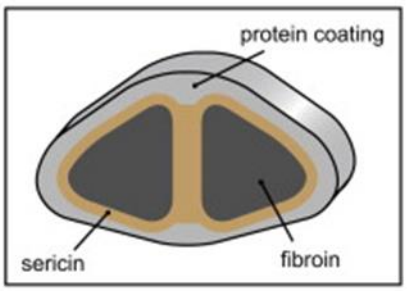


schematic top view

Figure 1. Electron micrograph and schematic illustration of silk fiber composed of silk fibroin (SF) and silk sericin (SS) [39].

SF attracts lots of attention as a biomaterial due to its unique structural characteristics and properties. Most protein materials used for biomedical applications are derived from tissues of allogeneic or xenogeneic origins. Such proteins have a potential risk for the infection from animal sources. On the other hand, SF protein, which is originated from insects, cocoon or spider web, might be safer than other animal protein sources. It has a good biocompatibility with minimal immunogenicity. It has been reported that the SF could be degraded into non-toxic products when implanted *in vivo* [44]. Most of all, unique structural characteristics and properties of SF, such as highly crystalline β-sheet structure and excellent mechanical property with high tensile strength can give better performance for end uses as a biomaterial. Potential risks of chemicals used for biomaterials fabrication might be a trouble when they are implanted into patient. Compared to other biopolymers, SF can be easily fabricated to various forms and shapes with insolubilization and crystallization simply by alcohol treatment, in which the alcohol is removed completely by washing and drying process. Therefore, the SF has a numerous potential in applications of biomedical fields.

In an economical point of view, cost of SF material is very low compared to other natural or synthetic biopolymers used in biomedical applications. Especially, in case of collagens, the raw material is very expensive due to its high cost and complexity of isolation and purification process. The SF can be simply purified from silkworm cocoons by weak alkaline treatment which

removes SS and other impurities. The processing cost for biomedical grade products is relatively low compared with that of other animal proteins. In addition, the SF annually has produced 1,000 metric tons per year in a world and the raw materials of SF can be easily obtained in a form of cocoons or fibers in a cheap price [2]. Such an economical advantage is favorable for a mass production of SF biomedical products.

## 2.2. DISSOLUTION AND REGENERATION OF SF

In general, SS is removed from silkworm cocoon by degumming process prior to use of silk fiber. This process is well known to textile industry for producing degummed silk fiber. Even when silk protein is used in biomedical applications, the soluble SS, which is coated on SF, should be removed before next regeneration step. Adequate removal of contaminating SS from silkworm silk may be required to avoid biocompatibility problems. It was reported that remained SS caused the immune response *in vivo* [43]. The SS can be removed easily by weak alkaline boiled solution. Sodium carbonate ($Na_2CO_3$) is mainly used for weak alkali reagent but sodium oleate ($CH_3(CH_2)_7CH=CH(CH_2)_7COONa$) is added to $Na_2CO_3$ in order to prevent the molecular weight decrease of SF. In severe conditions of degumming process, degradation of SF chain occurs and properties of SF is changed. Especially, SF can be damaged by long degumming process so that degumming time should be carefully controlled for a reproducibility of SF. When the degumming process is not properly carried out for a uniform degumming ratio, there are many difficulties in processing and the final SF products show different properties and performance.

The degummed SF has a well ordered crystalline structure with high crystallinity and orientation. Due to the hierarchical order in supramolecular structure and organization with high molecular weight, the SF is insoluble in water and most organic solvents. Truly, it is hard to dissolve the SF (usually in

a fiber form) without degradation. However, it has been known that highly concentrated salt solution (e.g., LiBr, $CaCl_2$,$CaNO_3$, etc.) were used for the dissolution of SF. The dissolution mechanism is that at a certain concentration condition, the salt effectively penetrates crystal regions of SF and disrupts hydrogen bonding of β-sheet structure [16]. After sufficient dialysis process, pure SF aqueous solution can be obtained and SF chains exist as a random coil conformation in the solution. It was reported that LiBr solvent system rarely damaged the SF molecular chains during dissolution process while $CaCl_2$ solvent system severely cleaved the SF chains [45]. In this reason, short dissolution time (within 3 min) is recommended for $CaCl_2$-based solvent system.

After dissolution and dialysis process, clear SF aqueous solution can be acquired. In general, freeze drying is conducted to make a sponge form of regenerated SF for further processing of SF into various forms. Because this regenerated SF is amorphous and consists of random coil conformation, it can be dissolved completely in acidic solvent (e.g., formic acid, trifluoroacetic acid, etc.) or fluorinated alcohol (e.g., 1,1,1,3,3,3-hexafluoro-2-propanol, etc.) [15, 46, 47]. Using suitable solvent systems, various types of regenerated SF, such as powder, particle, fiber, film, hydrogel, membrane, web, etc., can be fabricated for a proper application in biomedical field (**Figure 2**) [48]. Sponge type SF, which is fabricated by freeze drying of SF aqueous solution, is highly porous, providing a favorable environment in 3D for cell spreading,

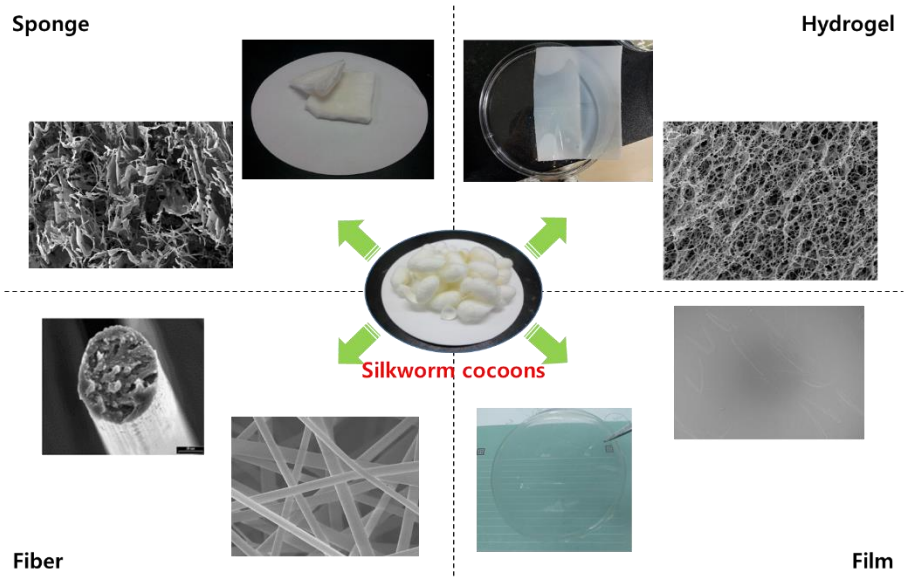


Figure 2. Typical regenerated forms of SF.

migration, and proliferation [49-51]. SF hydrogel is also easily fabricated using SF aqueous solution by forming of crosslinked network structure [6]. The hydrogel has a hydrophilic nature and highly porous structural environment in a wet condition, which can facilitate the 3D cell culture and cell encapsulation.

SF regenerated fiber can be fabricated by typical wet spinning process. When the SF dope solution is directly spun into a coagulation bath (precipitation in alcohol containing bath), several micron sized fiber can be obtained after stretching and drawing process [52, 53]. Electrospinning method can provide the fibers of several tens to hundreds of nanometer size in diameter, depending on the electrospinning conditions [54-56]. Especially, SF nanofiber web has a highly porous structure with interconnected fiber network. Porous structural features of this nanofibrous electrospun SF web can provide a favorable environment in cell culture and therefore, it has a high potential for a use in tissue engineering scaffold. Film or membrane can also be fabricated. After solvent casting and evaporation process, thin and transparent SF film were prepared and analyzed [57-59]. Solvent emulsion and electrospraying method were used for a fabrication of SF microsphere which had a small diameter within several tens of micron, being able to apply in drug delivery system [60-62].

## 2.3. SF HYDROGEL

### 2.3.1. General characteristics of hydrogel

Hydrogel is composed of 3D polymeric network which retains a large amount of water inside. According to a crosslinking mechanism, it is classified into two categories, physically crosslinked and chemically crosslinked hydrogel [6]. Polymeric network of physically crosslinked hydrogel is held together by secondary forces such as hydrogen bond, ionic bond, and hydrophobic interaction. On the contrary, chemically crosslinked hydrogel is linked by covalent bonds. Due to these polymeric network structures, hydrogel is basically elastic and possesses tremendous interconnected pores, in which lots of water molecules are entrapped. The main reason for wide applications of the hydrogel is close resemblance of its structural features and physical properties to those of biological tissues [63]. Highly porous 3D structure provides physiologically similar environment to cells that it has a potential in tissue engineering field.

### 2.3.2. Physically crosslinked SF hydrogel

#### 2.3.2.1. Gelation mechanism

Compared to other polymeric materials, SF chains can make physical crosslinking in solution state via hydrogen bonding formation, which is attributed to the structural transition of SF into insoluble β-sheet structure (**Figure 3**) [17, 18]. In solution state, a random coil conformation of SF is thermodynamically unstable, so that it prefers to be changed into stable β-sheet conformation. The structural transition is irreversible and hydrogel once formed cannot be recovered to original solution state. In addition to structural transition, aggregation and entanglement of SF molecular chains also plays a critical role in hydrogel formation. As a result of molecular chain association, it was reported that several tens of nanometer diameter of SF particles could be formed [64]. As gelation proceeds, these particles gradually aggregated into larger size by forming hydrogel network structure (**Figure 4**) [18, 29]. On a macroscopic level, the SF chains finally construct physically crosslinked network structure of hydrogel, which consists of β-sheet crystalline structure of SF. Due to its crystalline nature, SF hydrogel exhibits opaque optically [17].

#### 2.3.2.2. Strategies for hydrogel fabrication

Alcohols (e.g., methyl alcohol, ethyl alcohol, etc.) are mainly used for insolubilization of SF, which is attributed to promote its crystallization. When SF aqueous solution is treated with alcohols, water molecules are removed

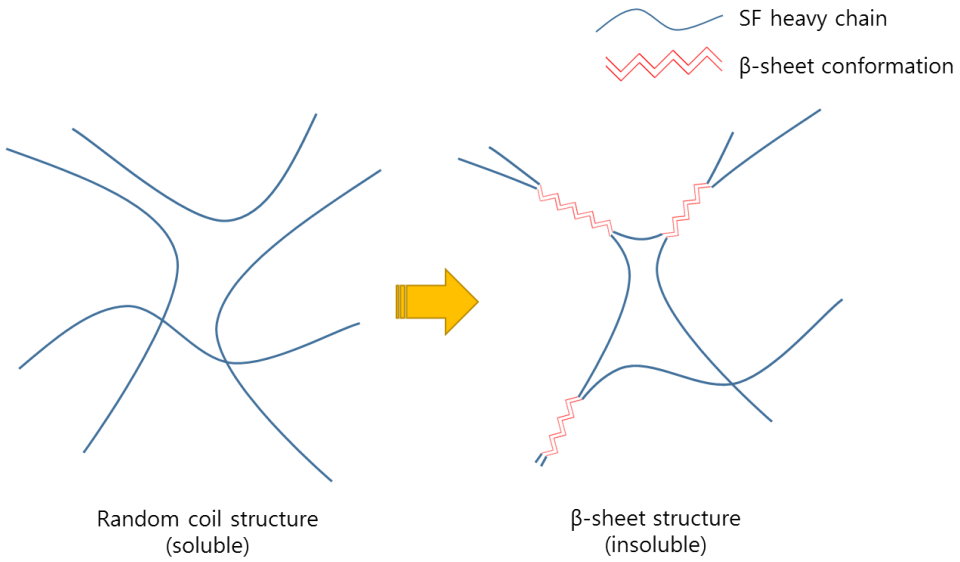


Figure 3. Schematic illustration of structural transition of SF molecular chains during gel formation.

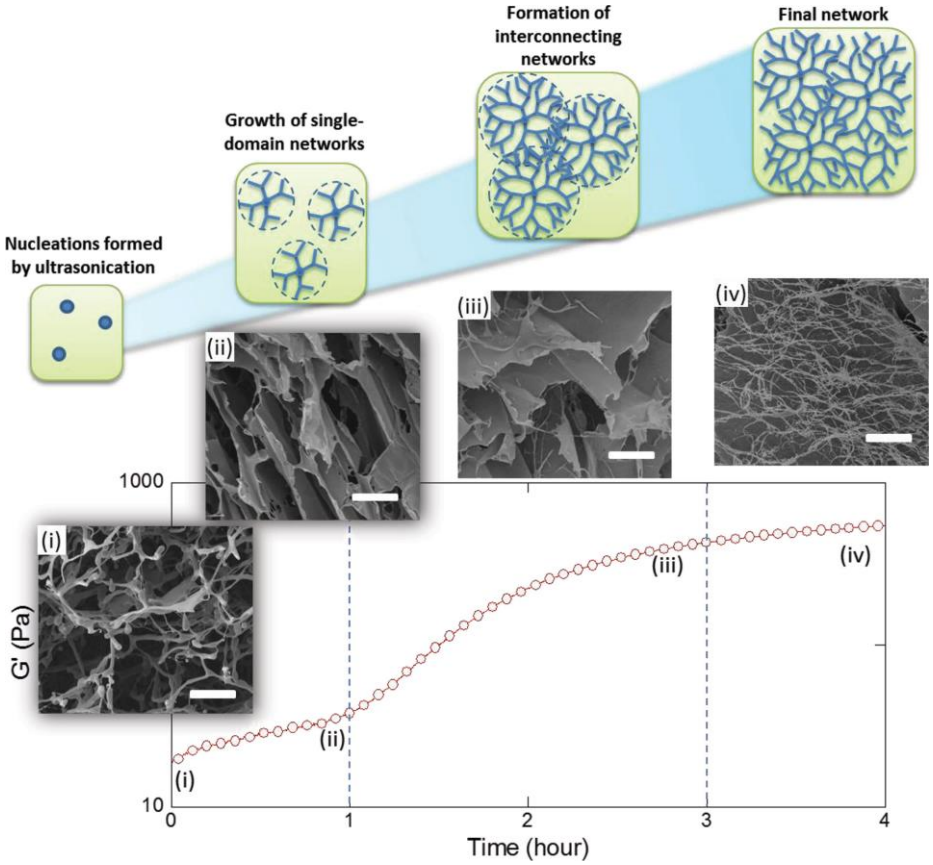


Figure 4. Illustration of the formation of nanofibrillar network at different gelation stages. Inserted SEM images represent freeze-dried RSF hydrogel at different gelation states: (i) 0 hr, (ii) 1 hr, (iii) 3 hr, (iv) 20 hr after ultra-sonication. The scale bar presents 500 μm [29].

temporarily from the SF chains (known as dehydration), which can facilitate the β-sheet structural transition of SF [65]. Such a transition occurs instantly in a very short time that alcohol induced SF hydrogel forms heterogeneous network structure mostly. Acetone was also used for a preparation of SF hydrogel in order to facilitate structural transition [66]. When the organic solvents are used for SF hydrogel fabrication, there might be a potential risk of cytotoxicity due to residual solvent remained.

Gelation temperature is an important factor for the gel formation. Gelation of SF aqueous solution can be promoted at high temperature condition. Because hydrophobic regions of SF tend to be separated from its hydrophilic regions at a relatively high temperature, the formation of aggregate becomes more preferable [64]. Such an aggregate formation is also affected by a concentration of SF aqueous solution. It is because possibility of molecular chain associations increase with an increment of concentration and aggregated/entangled regions are easily formed for gel formation [17, 19]. Another important parameter for affecting gel formation is pH. Physical crosslinking of SF is known to be facilitated at acidic condition [17]. At neutral pH condition (pH ~ 7), SF particles in aqueous solution have negative surface charges, which can interrupt the aggregation of SF due to a negative charge repulsion. On the other hand, possibility of chain aggregation increases when the pH of SF aqueous solution lowers to an isoelectric point of SF (pI ~ 4.3). Hence, the hydrogel formation of SF aqueous solution is preferable at an

acidic pH condition. Indirect method for controlling the pH of SF aqueous solution were proposed by M.L. Floren *et al*. and R.R. Mallepally *et al* [67, 68]. To acidifying the SF aqueous solution, they developed carbon dioxide ($CO_2$) gas bubbling technique for making SF hydrogel with unique structural characteristics. When $CO_2$ is applied to SF aqueous solution, $CO_2$ reacts with water to form carbonic acid ($H_2CO_3$). Protons ($H^+$) produced from $H_2CO_3$ finally lower the pH of the solution. Here, the applied $CO_2$ can acidify the whole part of SF aqueous solution, and as a result, homogeneous network structure of SF hydrogel is obtained.

In general, gelation conditions, such as temperature, concentration, pH, etc., should be adjusted for a proper gelation of SF. At ambient conditions, however, it takes several days or weeks for the gel forming. Therefore, it is necessary to accelerate gelation time so that gel formation can be done within 1 hour. It is well-known that hydrogel formation can be accelerated by external physical stimulation at same gelation conditions. Shear stress applying method, simply by tilting or agitating solution, is a mostly utilized strategy for shortening the gelation time of SF hydrogel. This stimulation can induce the aggregation of SF chains and promote the gel formation [21]. By controlling the amplitude and applying time of shear stress, both gelation time and gel strength of SF hydrogel were manipulated. However, a precise control of gelation behavior and physical property of hydrogel was impossible even though vortexing induced shear stress applying method used. It is because SF

chains prefer not a gel formation but a precipitation during vortexing treatment.

Ultra-sonication method is suggested as an alternative for making homogenous SF hydrogel structure. Not only ultra-sonication quickly induces gel transition of SF aqueous solution but also it can build up hydrogel network structure without precipitation [22, 69]. Similar to shear stress treatment, ultra-sonic wave highly enhances a frequency of molecule movement, which facilitates the aggregation of SF molecules. In addition, ultra-sonic wave can be distributed to whole parts of SF aqueous solution evenly so that this hydrogel has a homogeneous network structure with high mechanical strength and shear modulus. The ultra-sonication method also has a good reproducibility for hydrogel fabrication.

Electronic stimulation method was also introduced for the formation of physically crosslinked SF hydrogel [70, 71]. When the electric field applied to SF aqueous solution, a random coil conformation of SF changed to metastable state of α-helix conformation. Contrary to the shear stress applying method, such a structural transition can be temporarily recovered into a solution state if the applied electric field is removed. When the high voltage is applied to metastable state of SF, SF chains become elongated to the direction of current flow, resulting that α-helical conformation of SF changed to β-sheet conformation. This structural transition behavior finally constructs the physically crosslinked network of SF hydrogel.

In other way, additives can be used to induce and promote hydrogel formation. It was reported that poly(ethylene oxide) [19], poloxamer [72], N-lauroyl sarcosinate [73], glycerol [74], and sodium dodecyl sulfate [75, 76] were used as additives for SF hydrogel fabrication in order to promote the gelation of SF aqueous solution. The optimum amounts of additives exist for facilitating the gel transition of SF. This method has a limitation to be used because additional washing is required for removing residual additives from the hydrogel.

All the physical crosslinking methods utilized an innate structural characteristic of SF polymer in which hydrogel network structure was formed by self-aggregation of SF chains and structural transition of β-sheet conformation. Additional chemical modification or chemical crosslinker treatment are not required for the hydrogel formation. Therefore, only physically crosslinked SF hydrogel has a big advantage in biomedical applications due to its high biocompatibility. Nevertheless, there are some limitations remained for the use of this hydrogel. A brittleness, which is vulnerable to shear deformation (e.g., bending, twisting, etc.), is pointed out as one of drawbacks for the SF hydrogel. Poor mechanical property of physically crosslinked SF hydrogel may be due to inherently weak intermolecular hydrogen bonding against shear deformation in addition to a low degree of crystallinity of regenerated SF hydrogel [29]. To enhance the mechanical properties of SF hydrogel markedly, physical crosslinking is not

sufficient and consequently, introduction of chemical crosslinkers should be necessary for the better performance of the SF hydrogel.

### 2.3.3. Chemically crosslinked SF hydrogel

#### 2.3.3.1. General characteristics

Generally, chemically crosslinked hydrogel has more rigid and resilience mechanical property than physically crosslinked one. Besides, chemical crosslinking method can easily manipulate physical property of hydrogel in a wide range. It is because its property is mainly governed by crosslinking density of hydrogel. Such a crosslinking density can be modulated by controlling the input amount of crosslinker or amount of crosslinkable functional group of polymer. Many chemical crosslinking methods were proposed for the hydrogel fabrication of natural polymers. In case of SF hydrogel, SF polymer contains reactive functional moieties of hydroxyl (i.e., serine, tyrosine, and threonine), carboxyl (i.e., aspartic acid and glutamic acid), and amine (i.e., arginine and lysine) groups (**Table 1**) [1, 77]. **Figure 5** shows major functional groups of SF, which can be involved in chemical crosslinking reaction.

Compared to physical crosslinking, chemical crosslinking method has noticeable advantages for better performance of hydrogel. This method has a potential risk of cytotoxicity, however mechanical properties of chemically crosslinked hydrogel are superior due to network structural formation via intermolecular covalent bonds. Moreover, a gelation time can be controlled and predictable in chemical crosslinking. When this chemically crosslinked

Table 1. Amino acid composition of the heavy chain of silk fibroin [77].

| Amino acid | # Residues | Mol % |
|---|---|---|
| Ala (A) | 1593 | 30.3 |
| Arg (R) | 14 | 0.3 |
| Asn (N) | 20 | 0.4 |
| Asp (D) | 25 | 0.5 |
| Cys (C) | 5 | 0.1 |
| Gln (G) | 10 | 0.2 |
| Glu (E) | 30 | 0.6 |
| Gly (G) | 2415 | 45.9 |
| His (H) | 5 | 0.1 |
| Ile (I) | 13 | 0.2 |
| Leu (L) | 7 | 0.1 |
| Lys (K) | 12 | 0.2 |
| Met (M) | 4 | 0.1 |
| Phe (F) | 29 | 0.6 |
| Pro (P) | 14 | 0.3 |
| Ser (S) | 635 | 12.1 |
| Thr (T) | 47 | 0.9 |
| Trp (W) | 11 | 0.2 |
| Tyr (Y) | 277 | 5.3 |
| Val (V) | 97 | 1.8 |

Total number (#) of amino acids: 5263

Molecular weight: 391,593 Da

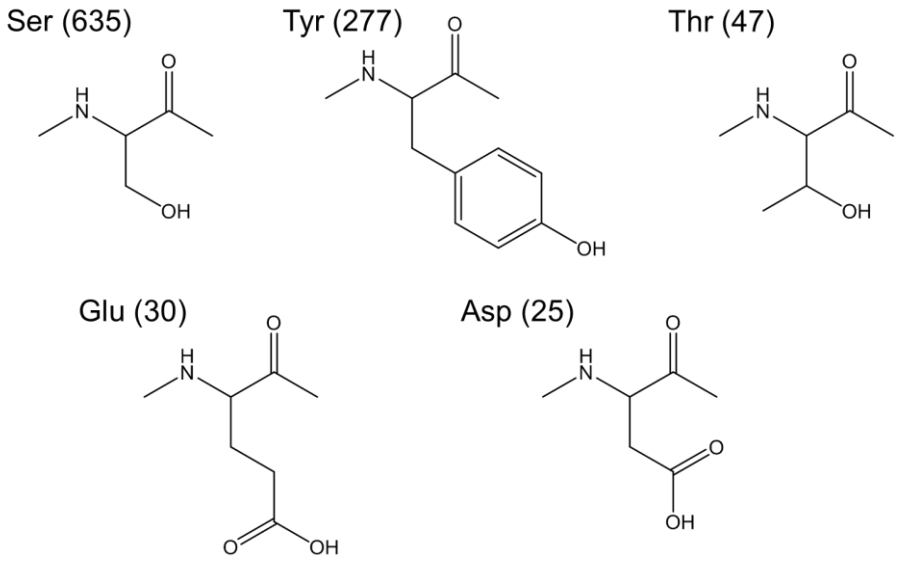


Figure 5. Chemical structures of most abundant reactive amino acids in SF. ( ): number of each residue among total number of amino acids, 5263.

hydrogel is used for biomedical applications, its biocompatibility should be evaluated and suitable fabrication method of this hydrogel should be also developed.

#### 2.3.3.2. Chemical crosslinkers

Among many chemical crosslinking agents, aldehyde type crosslinkers, such as formaldehyde, glyoxal, and glutaraldehyde, are mostly used for the crosslinking of proteins. It has been reported that amine groups of SF are participated in the crosslinking formation with high reaction yield when glutaraldehyde crosslinker was used in alkaline condition [32]. Even though the glutaraldehyde is frequently used for the crosslinking of SF, it is hard to make highly crosslinked network structure of SF hydrogel due to a low content of amine group (0.5 mol%) in SF. In acidic condition, on the contrary, hydroxyl groups, which are largest amount of reactive groups in SF protein (14.2 mol%), might be involved in chemical crosslinking by forming ether bond bridges between these groups for SF hydrogel fabrication. However, proper buffer solution is required to avoid precipitation of SF during crosslinking reaction.

Epoxide type crosslinkers are also popular for the chemical crosslinking formation of polymeric materials. Among them, epichlorohydrin and diglycidyl ether showed a high reactivity to link both of amine group and hydroxyl group of SF for hydrogel fabrication [30, 31, 33, 78]. Even though

these crosslinkers can easily make chemical crosslinked SF hydrogel, residual chemicals might have a toxicity problem and give a limitation of use in biomedical application. Moreover, this type of chemical reaction can lower the both of cell viability and drug activity when the cells and drugs are encapsulated in hydrogel network because of non-specific crosslinking reaction.

Often the chemical crosslinking method requires severe biological evaluations for the safety. Most of chemical crosslinkers are toxic and restricted to be used in biomedical fields. Nowadays, bioactive functional materials from natural sources tend to be used for the higher cytocompatibility. Genipin, which is a natural protein extracted from gardenia seeds (*Gardenia Jasminoides Ellis*), was introduced as a biocompatible crosslinker. W.H. Elliott *et al* reported a possible use of genipin, which could interlink amine groups of protein by covalent bond, for the fabrication of SF hydrogel [34]. The genipin crosslinker showed much lower cytotoxicity and its use in biomedical application was proposed. However, this type of crosslinking reaction requires long reaction time for hydrogel network formation, which makes some limitations to use, for example, in cell encapsulation.

Enzyme can be used for the crosslinking formation. In case of SF, tyrosinase-induced crosslinking pathways were proposed (**Figure 6**) [79]. SF contains about 5 mol% of tyrosine and this moiety can be crosslinked by tyrosine-based enzyme. When tyrosinase is added to SF aqueous solution,

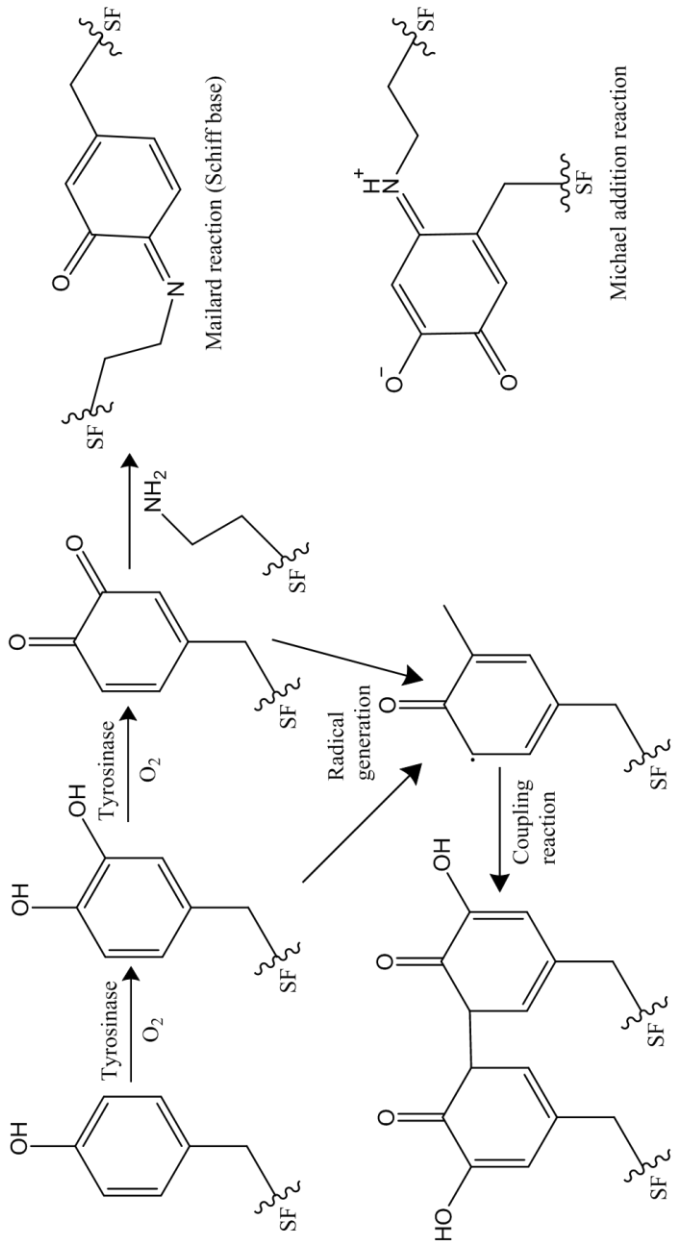


Figure 6. Proposed crosslinking reaction pathways for tyrosyl residues in SF molecular chains [79].

tyrosine residue of SF subsequently oxidized to dopa and dopaquinone. Final oxidized product, dopaquinone, can be reacted with amine group via Schiff-base reaction or same tyrosine group via Michael reaction by covalent bonding linkage. Such an enzyme-based chemical reaction is occurred at physiological condition, which makes an advantage in biomedical field. Moreover, crosslinking density can be controlled by amount of enzyme and dissolved oxygen. However, this enzyme-induced crosslinking still requires a longer reaction time for the hydrogel formation. Recently, B.P. Partlow *et al*. used horseradish peroxidase enzyme for chemical crosslinking of silk protein and developed highly tunable elastomeric functional SF hydrogel [35]. By increasing the concentration of dissolved oxygen, the chemical reaction could be completed within several minutes. Consequently, the gelation time was remarkably reduced and as a result, it was feasible to use the chemically crosslinked SF hydrogel in cell encapsulation.

#### 2.3.3.3. Photo-crosslinking system

As shown in enzyme-based chemical reaction methods, tyrosine residue is the mostly reactive functional group for the chemical crosslinking of SF. In the same way, photo-crosslinking method can be applied to the SF due to active photo-reaction of tyrosine groups. J.L. Whittaker *et al*. proposed facile and rapid ruthenium mediated photo-crosslinking of *Bombyx mori* SF for the fabrication of photo-crosslinkable SF hydrogel [80]. They used tris(2,2-bipyridyl) dichloro ruthenium (II) hexahydrate ($Ru(II)(bpy)_3^{2+}$) as a catalyst

and ammonium persulfate as an electron acceptor, respectively. Under visible light, $Ru(II)(bpy)_3^{2+}$ makes tyrosine radical. Subsequently, this radical reacts with another tyrosine and make di-tyrosine linkage. Covalent crosslinked SF hydrogel was successfully prepared but this hydrogel showed red light color due to the presence of $Ru(II)(bpy)_3^{2+}$. Recently, M.B. Applegate *et al*. reported new method for SF hydrogel fabrication via di-tyrosine linkage using photo-initiator [37]. Radicals produced from photo-initiator, riboflavin, made a covalent bonding between tyrosine residues of SF and this photo-crosslinked hydrogel showed highly transparent optical property, which can make possible to use for ocular prostheses. However, this reaction required longer reaction time compared to other photo-crosslinking reaction systems (more than 1 hr).

### 2.3.4. Biomedical applications of SF hydrogel

#### 2.3.4.1. Bone regeneration

SF hydrogel has been majorly developed as bone regenerative scaffold due to its rigid characteristic. M. Fini *et al*. reported a possible use of SF hydrogel as a bone scaffold [81]. They implanted the SF hydrogel in critical size cancellous defects of rabbit for 12 weeks and found new bone formation in SF hydrogel without immune reaction. P.H.G. Chao *et al*. also reported that SF hydrogel could promote the proliferation and differentiation of chondrocytes [82]. Compared to agarose hydrogel, SF hydrogel promoted the production of glycosaminoglycan and type II collagen from chondrocytes. To improve the resilience of SF hydrogel, M. Parkes *et al*. used poly (ethylene diglycidyl ether) for crosslinking of SF aqueous solution [33]. This crosslinker enhanced the mechanical property of SF hydrogel, which is sufficient for application in cartilage regeneration.

Bioactive materials were also blended with SF hydrogel for enhancing the bone regeneration. VEGF (vascular endothelial growth factor) and BMP-2 (bone morphogenic protein-2) were delivered to injectable sonication-induced silk hydrogel for regeneration of maxillary sinus floor [83]. These additives effectively promoted new bone formation. Bone major ingredient, hydroxyapatite, was also incorporated with SF hydrogel for bone regeneration. For a mineralization of hydroxyapatite, SF hydrogel was soaked in calcium

ion ($Ca^{2+}$) and phosphate ion ($PO_4^{2-}$) containing solution, alternatively [84]. After repeated soaking treatment, hydroxyapatite layer was coated on SF hydrogel and this could promote the proliferation and differentiation of human osteoblast like cells (MG-63). Hydroxyapatite nanoparticle containing SF composite hydrogels were also developed and evaluated for the performance [85, 86]. Homogeneous mixing or coating of nano-hydroxyapatites onto silk hydrogel is important for fabricating the composite material and this composite SF hydrogel showed an enhanced osteogenic induction and differentiation for bone regeneration.

### 2.3.4.2. Cell encapsulation

SF hydrogel can be applied as a cell encapsulation matrix only if gelation time is controlled within several minutes for hydrogel formation. Many studies were carried out for potential application of SF hydrogel in the use of cell encapsulation. Ultra-sonication is the easiest and most popular gelation facilitating method for fabricating physically crosslinked SF hydrogel. X. Wang *et al*. encapsulated mesenchymal stem cells (MSCs) in SF hydrogel matrix using ultra-sonication with high cell viability [22]. The MSCs were also co-encapsulated with splenocytes in SF hydrogel for enhancing the secretion of islet proteins [87]. W. Sun *et al*. successfully encapsulated neural stem cells (NSCs) in IKVAV peptide immobilized SF hydrogel [88]. It was found that laminin derived peptide, IKVAV, effectively promoted the growth of NSCs. Enzyme-based crosslinking method is another route for fabricating

the SF hydrogel and possible use in cell encapsulation was studied for this hydrogel matrix. B.P. Partlow *et al*. confirmed that MSCs could be survived during enzyme-induced SF hydrogel network formation, indicating that oxygen radicals rarely affect the viability of MSCs [35].

Other studies were also investigated for the use of SF hydrogel as stem cell culture matrix by blending with natural biopolymers in gel formation. According to Z. Gong *et al*. report, injectable thixotropic hydrogel comprising SF and hydroxypropyl cellulose (HPC) could be successfully fabricated for the use of cell encapsulation [89]. During gel formation (temperature transition), the cells were entrapped well in hydrogel network without any cell death. This is based on that HPC have a thermosensitive property and SF aqueous solution can form hydrogel at above temperature of lower critical solution temperature (LCST). K. Ziv *et al*. reported the alginate blended SF hydrogel scaffold for stem cell culture and transplantation [90]. When the SF/alginate blended aqueous solution was exposed to calcium ions, interpenetrating polymer network (IPN) structure was formed and embryonic stem cells (ESCs) could be encapsulated in SF/alginate hydrogel with a good cell viability.

### 2.3.4.3. Drug delivery

Due to its unique structures and physical properties, the hydrogel is frequently used in drug delivery system. During gel formation, drugs can be

easily loaded on the hydrogel network. There were several reports for the evaluation of SF hydrogels for drug delivery [91-93]. Crosslinking density of hydrogel is greatly affected by a concentration of precursor solution. In general, hydrogel made from high concentration precursor solution has dense hydrogel network structure, which interrupts the releasing of drug from the matrix. Lyophilized SF hydrogel was fabricated for the sustained local delivery of therapeutic monoclonal antibodies [92] and doxorubicin-loaded SF hydrogel for the focal treatment of primary breast cancer [94]. In case of doxorubicin-loaded SF hydrogel, it was injectable and showed the toxicity toward human breast cancer cells (MCF-7).

Compared to other polymeric hydrogels, the SF hydrogel is rarely swelled in water. Swelling property is the important factor for drug delivery matrix because entrapped drugs can be released well in loose (swelled) network structure. In this reason, synthetic polymers, such as poly (acrylamide) and poly (vinyl alcohol), were blended with SF for hydrogel formation [95, 96]. These blended SF hydrogel showed interpenetrating network structure for controlled drug release and the release rate could be increased due to enhancing swelling property of the hydrogel. It was also reported that SF/copolymer composite hydrogel was fabricated and evaluated. PLA-PEG-PLA tri-block copolymer was blended with SF for controlling release rate of hydrophilic/hydrophobic drugs from the composite hydrogel network [97].

#### 2.3.4.4. Miscellaneous

It was reported that gold nanoparticles embedded SF hydrogel (known as inorganic/organic hybrid hydrogel) was developed for treatment of skin infection [98]. When the gold nanoparticle was irradiated by laser beam, it produced the heat up to 60℃, which killed both of gram positive (+) (*Staphlococcus aureus*) and gram negative (-) (*Escherichia coli*) bacteria in subcutaneous. Therefore, focal infection treatment was achieved by using laser-mediated heating of injectable silk hydrogel with gold nanoparticles.

Recently, several trials were progressed to apply the SF hydrogel as ocular prostheses. When anti vascular endothelial growth factor (VEGF) loaded SF hydrogel was implanted to damaged cornea, it could suppress the vascularization without immune reaction [99]. In case of photo-crosslinked SF hydrogel prepared using riboflavin, it showed highly transparent optical property and greatly assisted the regeneration of cornea [37].

# III. MATERIALS AND METHODS

## 3.1. MATERIALS

*Bombyx mori* (*B.mori*) silkworm cocoons were obtained from NIAS, RDA (National Institute of Agricultural Sciences, Rural Development Administration) of Korea. *B.mori* silkworms were grown at Yeongdeok Taeyang Farm in Korea for obtaining medical grade silkworm cocoons.

Sodium oleate and calcium chloride were purchased from Tokyo Chemical Industry and Yakuri, respectively. Lithium bromide 1-hydrate and 2-isocyanatoethyl methacrylate were purchased from Kanto Chemical. The other chemicals were obtained from Sigma-Aldrich. All the reagents were used without further purification.

## 3.2. DISSOLUTION AND HYDROLYSIS OF SF

To remove SS, silkworm cocoons were boiled in 0.3% (w/v) sodium oleate and 0.2% (w/v) sodium carbonate cocktail solution at 100℃ for 1 hr. The SF aqueous solutions were obtained by using two different dissolving methods in this study. Especially, the hydrolysis and molecular weight control of SF were carried out using HAT method during the SF dissolution step. For LiBr-dissolution method, the degummed (SS removed) cocoons were dissolved in 9.3 M LiBr solution at 80℃ for 30 min. To hydrolyze SF, 0.6 M sodium hydroxide aqueous solution was directly added to the SF solution at a volume ratio of 1-to-5. Then, the final concentration of sodium hydroxide became 0.1 M in the SF solution. To control a molecular weight of SF, hydrolysis time was varied from 10 to 180 min, followed by subsequent dialysis against de-ionized water using cellulose acetate dialysis tube (MWCO: 12-14 kDa) for 3 days.

On the other hand, in case of $CaCl_2$-dissolution method, the degummed cocoons were dissolved in a ternary solvent of a $CaCl_2$/$dH_2O$/EtOH (molar ratio 1/8/2) at 80℃ for 5 min. The hydrolysis was directly performed at 80℃ for 10 to 120 min, followed by subsequent dialysis against de-ionized water using cellulose acetate dialysis tube (MWCO: 12-14 kDa) for 3 days.

## 3.3. FABRICATION OF SF HYDROGEL

### 3.3.1. Physically crosslinked SF hydrogel

After dialysis, SF solutions were centrifuged at 3,000 g for 10 min to remove insoluble aggregates. The final concentration of SF solution was in the range of 3.5-4% (w/v) and each solution was diluted to 3% (w/v) concentration. The prepared SF solutions were stored at 4℃ prior to gel fabrication process.

To initiate the gelation of SF solution, ultra-sonication was performed on 3% (w/v) SF aqueous solution of different molecular weights using an ultra-sonic processor (VCX-130, SONICS) at 32.5 W amplitude for 3 min. The treatment was conducted in an ice chamber to prevent the heat elevation during ultra-sonication. Then, ultra-sonicated SF solution was filtered and incubated at 60℃ for 2 days for preparing physically crosslinked SF hydrogel. The detail preparation conditions and sample ID were listed in **Table 2** and **Table 3**.

Table 2. Sample ID and preparation conditions of alkali hydrolyzed SF solutions using LiBr-HAT method.

| Sample ID | Dissolution condition | Dissolution time (min) | Hydrolysis condition | Hydrolysis time (min) |
|---|---|---|---|---|
| L0 | Solvent: 9.3 M LiBr<br>Temperature: 80℃<br>Liquor ratio: 1 g/ 5mL | 30 | Alkali: 0.1 M NaOH<br>Temperature: 80℃ | 0 |
| L10 | | | | 10 |
| L30 | | | | 30 |
| L90 | | | | 90 |
| L180 | | | | 180 |

Table 3. Sample ID and preparation conditions of alkali hydrolyzed SF solutions using $CaCl_2$-HAT method.

| Sample ID | Dissolution condition | Dissolution time (min) | Hydrolysis condition | Hydrolysis time (min) |
|---|---|---|---|---|
| C0 | Solvent: $CaCl_2$/$dH_2O$/EtOH (1/8/2) Temperature: 80℃ Liquor ratio: 1 g/5 mL | 5 | Alkali: 0.1 M NaOH Temperature: 80℃ | 0 |
| C10 | | | | 10 |
| C30 | | | | 30 |
| C60 | | | | 60 |
| C120 | | | | 120 |

### 3.3.2. Chemically photo-crosslinked SF hydrogel

After dialysis, SF solutions were centrifuged at 15,000 g for 20 min to remove insoluble aggregates. Then, supernatant was freeze-dried and stored at 4℃ prior to chemical modification of SF. To synthesize SFMA, previously reported method for methacrylate-functionalized SS was applied [38]. Briefly, the hydrolyzed SF was dissolved in 1 M lithium chloride (LiCl) dissolved dimethyl sulfoxide (DMSO). Subsequently, 2-isocyanatoethyl methacrylate (IEM) was directly added to the SF solution at 60℃ for 5 hr under nitrogen atmosphere (**Figure 7**). The final concentrations of SF and IEM in the reaction solution were 5 wt% and 0.25-2 mmol per 1 g of SF, respectively. Then, the solution was diluted with 10 × volume de-ionized water and dialyzed against de-ionized water at room temperature for 3 days using cellulose acetate tube (MWCO: 12-14 kDa). After dialysis, SFMA solutions were centrifuged at 15,000 g for 20 min to remove insoluble aggregates. Then, supernatant was freeze-dried and stored at 4℃ until gel fabrication.

For preparing precursor solutions, SFMA and 1mM lithium phenyl-2,4,6-trimethylbenzoylphosphinate (LAP) were dissolved in pH 7.4 phosphate buffered saline (PBS) with varying SFMA concentrations (10 to 20 wt%). After vortexing, the solution was placed in the gap between two glass slides (gap size: 1 mm), followed by UV light irradiation (5 $mW/cm^2$, 365 nm) for 5 min (**Figure 8**). Finally, SFMA hydrogel slabs were punched out by an 8 mm biopsy punch.

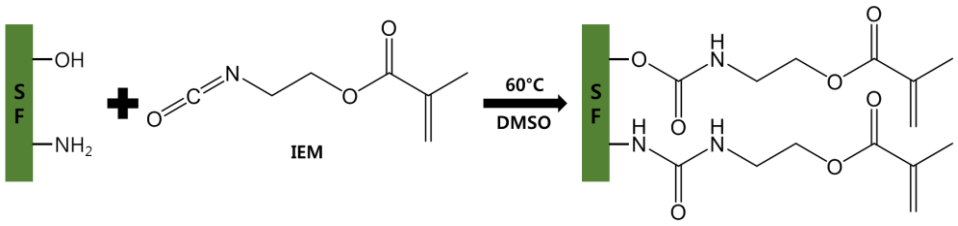


Figure 7. Reaction scheme for the synthesis of hydrolyzed silk fibroin methacrylate (SFMA) using IEM.

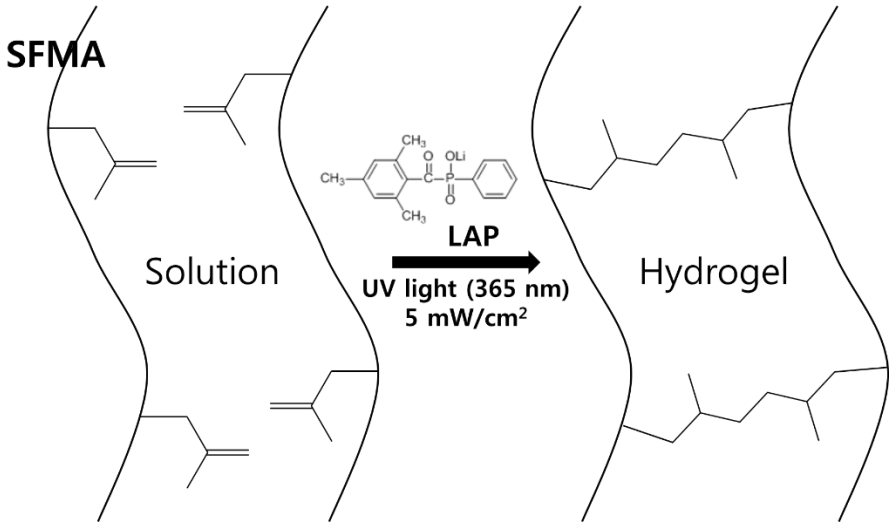


Figure 8. Schematic of hydrolyzed silk fibroin methacrylate (SFMA) hydrogel formation under UV irradiation.

## 3.4. PROPERTY MEASUREMENT AND ANALYSIS

### 3.4.1. Molecular weight of SF

The molecular weight of SF was measured by gel filtration chromatography (GFC) (AKTA Purifier, GE Healthcare) with Superdex 200 10/300 GL column (GE Healthcare). 0.5 mL of 3% (w/v) SF solution was added to 4 mL of 6 M urea aqueous solution, followed by filtration with 0.2 μm membrane. For the measurement, 300 μL of sample solution was injected and 1.5 column volume of 4 M urea was eluted at a constant flow rate of 0.5 mL/min. The elution of SF was detected by UV detector at 280 nm wavelength. The molecular weight of SF was determined by a calibration curve, which was obtained by a standard globular protein kit (Gel Filtration Cal Kit High Molecular Weight, GE Healthcare).

### 3.4.2. Qualitative analysis of SFMA

The amount of MA immobilized on SF and reaction yield were measured by $^{1}$H NMR (600 MHz, Bruker) with an aid of amino acids composition analysis using high performance liquid chromatography (HPLC) (UltiMate® 3000, Dionex™, Thermo Fisher Scientific). Acid hydrolysis was conducted for obtaining hydrolysates for amino acids composition analysis. Reaction yield was calculated by following Eq. (1), (2), and (3). The peak areas in Eq. (3) could be calculated by integrating the peaks at 6.5-7.5 from Tyr 4H and the peaks at 6.13 and 5.72 ppm from the double bond hydrogens of methacrylate group [100, 101].

$$\text{Reaction yield (\%)} = \frac{Immobilized\ IEM\ concentration\ per\ 1\ g\ of\ SF\ \cdots(Eq.(2))}{Input\ IEM\ concentration\ per\ 1\ g\ of\ SF} \times 100 \quad (1)$$

$$\text{Immobilized IEM concentration per 1 g of SF (mmol)} = mole\ concentration\ of\ 1\ g\ SF\ \times the\ number\ of\ Tyr\ in\ SF \times \frac{Eq.(3)}{100} \quad (2)$$

$$\text{Mole\% of MA in SF} = \frac{Peak\ area\ of\ MA\ 2H/2}{Peak\ area\ of\ Tyr\ 4H/4} \times mol\%\ of\ Tyr\ in\ SF \quad (3)$$

### 3.4.3. Swelling behavior of SF hydrogel

#### 3.4.3.1. Gel fraction

For physically crosslinked SF hydrogel, each gel was dried at 60℃ for 24 hr in vacuum right after the fabrication and its initial dry-weight ($W_{d0}$) was measured. The dried gels were incubated in de-ionized water at 37℃ for 24 hr and washed several times. The swollen gels were then re-dried in vacuum for 24 hr and its dry-weight ($W_{d1}$) was measured. The gel fraction was obtained by Eq. (4).

$$\text{Gel fraction } (\%) = \frac{W_{d1}}{W_{d0}} \times 100 \qquad (4)$$

For chemically photo-crosslinked SF hydrogel, gel fraction was determined using following Eq. (5) by measuring a weight of dried hydrogel ($W_d$) after washing in deionized water for 24 hr at 37℃ for removal soluble fractions.

$$\text{Gel fraction } (\%) = \frac{W_d}{W_t} \times 100 \qquad (5)$$

where $W_t$ is the theoretical weight of SFMA participated in hydrogel network.

#### 3.4.3.2. Swelling ratio

For physically crosslinked SF hydrogel, each gel was incubated in pH 7.4 PBS at 37℃ for 24 hr. Then, the samples were weighted to obtain swollen weight of hydrogel ($W_s$). The swollen hydrogels were washed to remove the

residual ions of PBS for 24 hr using de-ionized water, followed by vacuum drying and then, dry weight ($W_d$) was measured. The equilibrium mass swelling ratio of SF hydrogel was defined as following Eq. (6).

$$\text{Swelling ratio (q)} = \frac{W_s}{W_d} \qquad (6)$$

In case of chemically photo-crosslinked SF hydrogel, each gel was incubated in pH 7.4 PBS at 37℃ for 24 hr. The equilibrium mass swelling ratio of SF hydrogel was defined as following Eq. (7).

$$\text{Swelling ratio (q)} = \frac{W_{s1}}{W_{s0}} \qquad (7)$$

where $W_{s0}$ and $W_{s1}$ are weight of swollen hydrogel measured at day 0 and 1, respectively.

### 3.4.4. Rheological behavior of SF hydrogel

#### 3.4.4.1. Gel point

For physically crosslinked SF hydrogel, shear elastic and loss moduli (G′ and G″) were measured using a rheometer (HAAKE MARS III, Thermo Fisher Scientific) over the SF solution incubation time after ultra-sonication. The measurement was performed using a time-sweep oscillatory mode (strain: 5%, frequency: 1 Hz, gap size: 100 μm) with parallel plate geometry (Dia.: 35 mm). All the solutions were stored at 60℃ before measurement.

On the other hand, in case of chemically photo-crosslinked SF hydrogel, in situ photo-rheometry was conducted using a digital rheometer. It was operated in a time-sweep oscillatory mode (strain: 5%, frequency: 1 Hz, gap size: 100 μm) with a UV cure cell at room temperature using parallel plate geometry (Dia.: 35 mm). A precursor solution was placed on a quartz plate in the UV cure cell and irradiated with UV light (Omnicure S1000, 365 nm, 5 $mW/cm^2$) via liquid light guide. UV light was turned on 60 sec after the onset of rheometrical measurements. The gel point is defined as a specific time point when elastic modulus (G′) surpasses viscous modulus (G″).

#### 3.4.4.2. Equilibrium shear elastic modulus

The swollen SF hydrogel was punched out using a biopsy punch (8 mm). Then, shear elastic modulus (G′) was measured by the rheometer using a strain-sweep oscillatory mode (strain: 0.1-10%, frequency: 1 Hz, gap size: 1-

2.5 mm) with parallel plate geometry (8 mm). After the measurement, G' was determined from linear viscoelastic region.

### 3.4.4.3. Degradation kinetic

Degradation kinetic was also tracked by measuring the G′ of SFMA hydrogels incubated in PBS at 37℃ for 1 to 48 days. Degradation rate constant (k') was obtained from initial linear slope of following Eq. (8)

$$-k't = ln\frac{G'_t}{G'_1} \qquad (8)$$

where $G'_1$ and $G'_t$ are the G′ of swollen hydrogel measured at day 1 and t, respectively.

### 3.4.4.4. Thixotropic property

To measure thixotropic property of SFMA hydrogel, shear elastic and loss moduli (G′ and G″) were measured by a rheometer, which was operated in a stress-sweep oscillatory mode (stress: 0.1 to 500 Pa, frequency: 1 Hz, gap size: 1 mm) with a parallel plate geometry (Dia.: 8 mm). Also, 300 and 0.1 Pa of stress were alternatively applied to measure reversible thixotropic property of the hydrogel for 200 sec.

### 3.4.5. Structural characterization of SF hydrogel

#### 3.4.5.1. Fourier transform infrared spectroscopy

The secondary structure content of SF hydrogel was analyzed by attenuated total reflectance Fourier transform infrared spectroscopy (ATR FT-IR) (Nicolet 6700, Thermo Scientific, USA). For sample preparation, SF hydrogels were freeze-dried to prevent the structural deformation. Then, dried samples were measured in an amide I region (1700-1600 $cm^{-1}$) with 128 scan number at 8 $cm^{-1}$. Peak deconvolution was conducted using Origin Pro 8.0 and each content of secondary structure of SF (e.g., β-sheet, random coil) was calculated [102].

#### 3.4.5.2. Thioflavin T assay

The β-sheet formation of SF hydrogel was monitored by thioflavin T assay. For sample preparation, 990 μL of ultra-sonic wave treated SF solutions were mixed with 10 μL of 2 mM thioflavin T aqueous solution and prepared in 96 well-plate. Fluorescence was measured (ex/em: 450/485 nm) using a microplate reader (Synergy HT, Bio-Tek instruments). All the samples were stored at 60℃ before measurement.

#### 3.4.5.3. Visible light transmittance

For physically crosslinked SF hydrogel, 3% (w/v) SF solution was transferred into polystyrene UV/Vis spectrometry cuvette and each cuvette was completely sealed. To measure the turbidity, SF hydrogels were formed in

the same cuvette by ultra-sonication and subsequent incubation at 60℃ for 2 days. The transmittance was measured in a range between 400 to 700 nm by using UV/Vis spectrometer (OPTIZEN POP, Mecasys). The path length was fixed at 10 mm.

For chemically photo-crosslinked SF hydrogel, 100 μL of 12.5 wt% SFMA precursor solution was transferred into 96 well-plate. The transmittance was measured in the range between 400 to 800 nm by microplate reader (Synergy HT, Bio-Tek instruments).

### 3.3.5.4. Wide angle X-ray diffraction

Wide angle X-ray diffraction (WAXD) method was used for examining crystal structure of SF hydrogel. X-ray diffractogram was obtained by two theta (2θ) scanning with a GADDS (general area detector diffraction system, Brucker-Axs) using Cu Kα X-ray (1.54Å) at 40 kV and 45 mA irradiation conditions.

### 3.4.5.5. Small angle X-ray scattering

The microstructure of SF hydrogel was analyzed by using a small angle X-ray scattering (SAXS) spectrophotometer (TVXA-ENIF1, Techvalley). Wetted-samples (original hydrogel formation) of physically crosslinked SF hydrogel were used for the SAXS analysis. The distance from sample to detector was 1 m and the X-ray wavelength was 1.54 Å. Each SAXS pattern was collected for 10,000 s and converted to the scattering function $I(q)$ as a

function of the magnitude of the scattering vector ($q$).

For chemically photo-crosslinked SF hydrogel, the microstructure of SFMA hydrogel was analyzed by using a SAXS spectrophotometer (NANOSTAR, Bruker). 2 mm-thick hydrogels, after incubated in PBS at 37℃ for 24 hr, were used for the SAXS analysis. Each SAXS pattern was collected for 600 s and converted to the scattering function $I(q)$ as a function of the magnitude of the scattering vector $(q)$.

At a low $q^2$ region ($q^2$ < 0.024 nm), radius of gyration ($R_g$) was derived from Guinier equation (Eq. (9)), where $I_G(q)$ is the asymptotic value of the Guinier intensity at $q \rightarrow 0$. The $R_g$ value was calculated from the slope value of Guinier plot ($q^2$ versus $\ln(I_G(q))$.

$$I_G(q) = I_G(0)\exp(-q^2 {R_g}^2/3) \quad (9)$$

Then, Kratky plot was applied as a function of q versus $q^2 I(q)$.

### 3.4.5.6. Circular dichroism

The secondary structure of SF and SFMA solutions was analyzed by circular dichroism (CD) spectroscopy. For sample preparation, SF and SFMA were dissolved in PBS for 1 hr at 0.1% (w/v) concentration. Then, CD spectra were obtained in the far-UV region (195 to 245 nm) using a CD detector (Chirascan plus, AppliedPhotophysics).

### 3.4.5.7. Field emission scanning electron microscope

Field emission scanning electron microscope (FE-SEM, SUPRA55VP, Carl Zewiss) was used for examining morphological structure of SF hydrogel. To prepare sample, SF hydrogel was frozen at −70℃ overnight and lyophilized. Then, cross-section of drying samples was coated by platinum sputter coater (BAL-TEC/SCD 005, BAL-TEC) at 20 mA for 150 sec before FE-SEM observation.

### 3.4.6. Resilience measurement

Resilience of SFMA hydrogels was measured by using universal testing machine (LRX plus, LLOYD INSTRUMENTS), operated in a cyclic compressive mode. 2 mm-thick SFMA hydrogels were incubated in PBS at 37℃ for 24 hr. Then, circular gel discs (Dia.: 8 mm) were punched out from the gel slabs using a biopsy punch. 50 times of cyclic compressive tests were performed under a cross-head speed of 5 mm/min at ambient conditions. For a comparison with physically crosslinked SF hydrogel, molecular weight of SF and G′ value were fixed between the samples (G′ ~ 1.3 kPa). For preparing physically crosslinked SF hydrogel, ultra-sonication was performed on 3% (w/v) SF aqueous solution with 3 hr hydrolyzed sample (100 kDa) using ultra-sonic processor (VCX-130, SONICS) at 32.5 W amplitude for 3 min.

## 3.5. BIOLOGICAL EVALUATION OF SF HYDROGEL

### 3.5.1. Cell culture and sample preparation

#### 3.5.1.1. Physically crosslinked SF hydrogel

Human mesenchymal cells (hMSCs) were cultured in low glucose DMEM (Dulbecco modified eagle's medium, low glucose) supplemented with 10% (v/v) FBS (fetal bovine serum), 1% (v/v) antibiotic-antimycotic and 1ng/mL bFGF (basic fibroblast growth factor) at 5% $CO_2$ and 37℃. Before cell seeding, the SF hydrogels of different SF molecular weights were prepared in 48 well-plate by following the previously described method in 'section 3.3.1.'. For sample sterilization, SF aqueous solutions were filtered using 0.2 μm membrane before gel fabrication. Then, the cells were trypsinized with 0.25% trypsin-EDTA solution and hMSC cells of 15,000 were seeded on the top of each hydrogel. The seeded hMSCs were cultured in medium for 24 hr at 5% $CO_2$ and 37℃.

#### 3.5.1.2. Chemically photo-crosslinked SF hydrogel

Mouse fibroblast (NIH-3T3) cells were cultured in high glucose DMEM supplemented with 10% (v/v) FBS and 1% (v/v) antibiotic-antimycotic at 5% $CO_2$ and 37℃. Then, cells were trypsinized with 0.25% trypsin-EDTA solution and NIH-3T3 cells of 10,000 were seeded on the 96 well-plate. The seeded NIH-3T3 cells were cultured in medium for 24 hr at 5% $CO_2$ and 37℃.

To extract soluble materials from the hydrogel, 0.1 g of SFMA hydrogels (25_1.0 and 100_1.0) were incubated in serum free DMEM for 24 hr at 37℃ (1× relative concentration). After removing cell culture medium from the 96 well-plate, cells were cultured in various concentrations (0.5 to 0.0156× relative concentration) of the hydrogel extracts contained medium for 24 hr at 5% $CO_2$ and 37℃. Serum free DMEM was used as a negative control.

### 3.5.2. Cell morphology

The hMSCs on physically crosslinked SF hydrogel were observed using a microscope (Olympus CKX41, Olympus). Fluorescence images of hMSCs on the SF hydrogels were obtained using a confocal laser scanning microscope (CLSM) (SP8 X STED, Leica). The hMSCs were visualized 1-day post-seeding. Cell-attached hydrogels were fixed in 4% paraformaldehyde at room temperature for 10 min. Then, samples were rinsed with PBS and seeded cells were permeabilized with 0.25% Triton X-100, followed by blocking with 1% BSA in PBS containing 0.05% Tween20 at room temperature for 30 min. The samples were subsequently stained using rhodamine phalloidin (Molecular Probes®) and DAPI dihydrochloride (Molecular Probes®) for 15 min and washed with PBS.

### 3.5.3. Metabolic activity

Metabolic activity of hMSCs cultured on physically crosslinked SF hydrogel and NIH-3T3 cells cultured on TCP were measured by CellTiter-Blue® assay (Promega), respectively. Briefly, CellTiter-Blue® 10× reagent was diluted into FBS-contained DMEM at 10% (v/v). Then, 500 μL of 1× CellTiter-Blue® reagent was added into each well after removing old culture medium, followed by incubation at 5% $CO_2$ and 37℃ for 2 hr. 200 μL of reduced 1× CellTiter-Blue® reagent was transferred to 96-well plate for fluorescence measurement (ex/em: 560/590 nm) using a microplate reader (Synergy HT, Bio-Tek instruments).

The relative cell viability was obtained by following Eq. (10).

$$\text{Relative cell viability (\%)} = \frac{F_H}{F_S} \times 100 \qquad (10)$$

where $F_S$ and $F_H$ are the fluorescence intensity of NIH-3T3 cells cultured serum free medium and hydrogel extracts contained medium, respectively.

# IV. RESULTS AND DISCUSSION

## 4.1. PHYSICALLY CROSSLINKED SF HYDROGEL

### 4.1.1. Molecular weight control of SF

The solubilized SF molecules are able to form hydrogel network structure by a so-called self-assembly mechanism, in which the physical crosslinking occurs between hydrophobic segments of SF. Such a physical crosslinking can be initiated or accelerated by various external stimuli, such as shear force, electric current, and ultra-sonication in physiologically preferred condition [21, 22, 70]. Therefore, the fabrication process and properties of SF hydrogels have been widely explored especially for biomedical purposes. Nevertheless, the properties of SF hydrogel were not much variable due to the distinct characteristics of SF.

In this study, to manipulate the physical properties of SF hydrogel, the hydrolysis of SF molecules by heat-alkaline treatment (HAT) was applied, resulting in a change of average molecular weight as well as distribution of SF molecules. At first, availability of HAT was evaluated on generally-known two dissolution methods (i.e., LiBr and $CaCl_2/dH_2O/EtOH$ solvent system). By regulating HAT time, similar number average molecular weight ($M_n$) and polydispersity index (PDI) values of hydrolyzed SF could be obtained for both solvent systems. The range of $M_n$ was 77.2 to 258.6 kDa for LiBr and 73.1 to 252.5 kDa for $CaCl_2$, respectively (**Table 4**).

Table 4. Number average molecular weight ($M_n$) and polydispersity index (PDI) of hydrolyzed SF aqueous solutions measured by GFC.

| Sample ID | $M_n$ | PDI | Sample ID | $M_n$ | PDI |
|---|---|---|---|---|---|
| L0 | 258,600 | 1.39 | C0 | 252,500 | 1.43 |
| L10 | 215,700 | 1.61 | C10 | 196,700 | 1.69 |
| L30 | 182,200 | 1.83 | C30 | 136,800 | 2.15 |
| L90 | 123,700 | 2.01 | C60 | 105,500 | 2.09 |
| L180 | 77,200 | 3.09 | C120 | 73,100 | 3.12 |

However, in case of $CaCl_2$-HAT dissolution and hydrolysis method, the resulted SF solutions were not able to form a hydrogel (**Table 5**). Even though the $M_n$ of C10 ($M_n$: 196.7 kDa) was higher than that of L30 ($M_n$: 182.2 kDa), as shown in **Table 4**, C10 sample could not form hydrogel network structure. It seems that most of physically crosslinkable part of SF chain was cleaved during $CaCl_2$-HAT process. It is because $CaCl_2$ can easily infiltrate to the hydrophobic segment of SF more than LiBr by disrupting the main repeating amino acid unit of SF [45]. In this reason, SF aqueous solution made of $CaCl_2$ method showed a high turbidity, which had a several hundred micron size of SF particles for visible light scattering [45]. Hence, the LiBr-HAT dissolution-hydrolysis method was finally adopted to fabricate SF hydrogels of different molecular weights.

**Figure 9A** revealed molecular weight distributions of hydrolyzed SF with different HAT times. The intact SF (L0) showed a relatively narrower single peak at around 8.2 mL (~443 kDa), which is attributed to the molecular weight of SF heavy chain. As the hydrolysis time increased, the first shoulder peak at 9.5 mL (~200 kDa) appeared. With further time progression, the second shoulder peak developed at 14.0 mL (~17 kDa) while intensity of the intact SF peak at 8.2 mL gradually decreased. During alkali hydrolysis, the $M_n$ of SF decreased from 77.2 to 258.6 kDa while the PDI increased up to 3.1 at 180 min (**Figure 9B**). This indicates that the LiBr-HAT method is very useful for controlling the $M_n$ of SF in a wide range.

Table 5. Gel forming ability of ultra-sonicated SF aqueous solutions.

| Sample ID | Gel formation | Sample ID | Gel formation |
|---|---|---|---|
| L0 | ○ | C0 | ○ |
| L10 | ○ | C10 | × |
| L30 | ○ | C30 | × |
| L90 | ○ | C60 | × |
| L180 | ○ | C120 | × |

○: hydrogel formation completes, ×: no hydrogel formation and precipitation occurs.

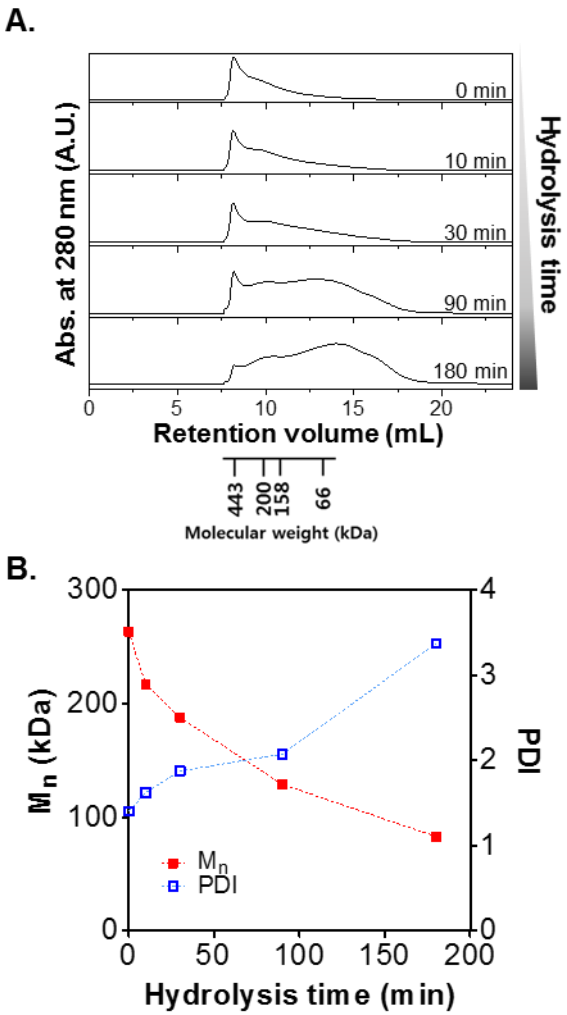


Figure 9. (A) Gel filtration chromatograms, and (B) number average molecular weight ($M_n$) and polydispersity index (PDI) of alkali hydrolyzed SF by HAT.

### 4.1.2. Gelation behavior of SF hydrogel

Rheological behavior of ultra-sonication treated SF solutions was examined for comparing $M_n$ effect on the gel forming aspect of SF hydrogel. **Figure 10A** shows shear moduli (G′ and G″) of 3% (w/v) SF solutions hydrolyzed for a different time (0 to 180 min) right after the ultra-sonication. G′ was higher than G″ in intact SF solution (L0), exhibiting the typical gel state (**Figure 10Aa**). In contrast, G′ was slightly lower than G″ in hydrolyzed SF solution (L180), indicating that the SF solution still maintained the sol state (**Figure 10Ae**). And the other samples (L10, L30, and L90) of different hydrolysis time also showed the sol state (**Figure 10Ab, 10Ac, and 10Ad**). These mean that hydrolyzed SF solutions remained sol state after ultra-sonication.

To determine the gel point, ratios of G′ to G″ were obtained as a function of incubation time at 60℃ for all the SF solutions. The gel state was determined when the ratio (G′/G″) surpassed 1, as shown in **Figure 10B**. In all samples, G′/G″ increased with incubation time. Especially for sample L0, the G′/G″ was about 7 even though it was not stored at 60℃ incubator. However, increment rate of G′/G″ value became slow as the $M_n$ of SF decreased. For example, sample L180 took 7 times longer time to reach the same value (G′/G″ = 3) than L10. The gel point of each hydrolyzed SF solution was presented in **Figure 10C**. Such an increment of gelation time was mainly attributed to the destruction of hydrophobic segments of SF. Both A. Matsumoto *et al*. and

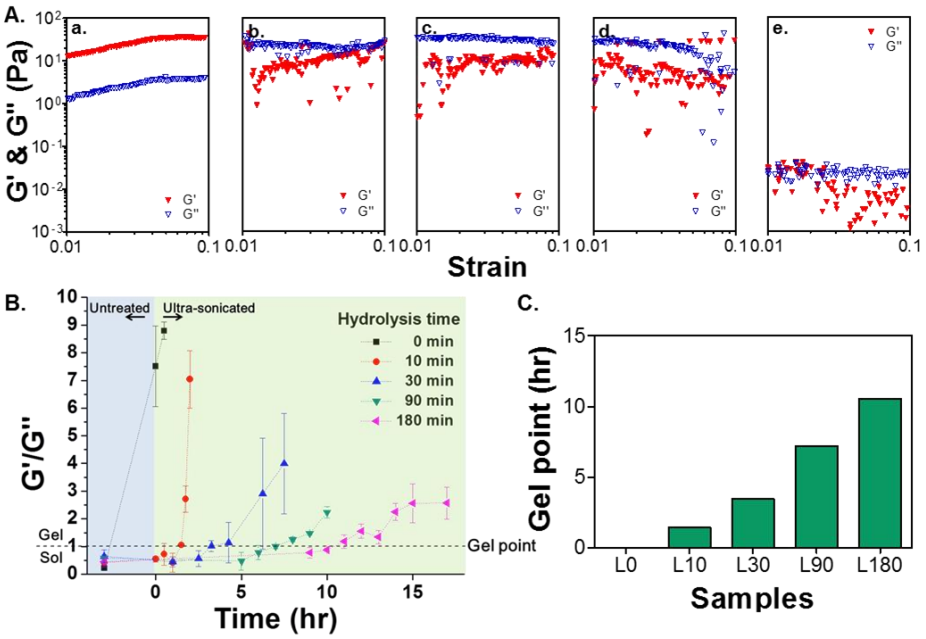


Figure 10. (A) Shear elastic and loss moduli (G' & G") of un- (a), 10 min- (b), 30 min- (c), 90 min- (d), and , 180 min- (e) hydrolyzed 3% (w/v) SF solutions immediately after ultra-sonication. (B) G'/G" ratio change of SF solutions with incubation time (a G′/G″ ratio larger than 1 indicates gel state, mean ± SD, n = 3). (C) Gel point (time when G'/G" = 1) of SF aqueous solutions formed of different molecular weights of SF.

S. Nagarkar *et al*. reported that free SF chains build physical crosslinks via β-sheet structure formation by intermolecular hydrogen bonding during the sol-gel transition [17, 18]. It is due to that the hydrophobic segment (Gly-Ala-Gly-Ala-Gla-X, X = Ser or Tyr) of SF plays a key role in the crosslinking.

Here, FT-IR analysis and thioflavin T assay were conducted to compare β-sheet content of SF hydrogel formed of different molecular weights of SF. It has been known that these are useful analysis techniques for comparing β-sheet content of SF [102, 103]. In particular, thioflavin T assay is the powerful tool for quantifying the β-amyloid structure (e.g., β-sheet) content [104, 105], which is based on that thioflavin T selectively infiltrates to anti-parallel β-sheet structure and illuminates the green fluorescence. **Figure 11A** shows FT-IR spectra of SF hydrogels formed of different molecular weights of SF. In general, SF protein exhibits typical FT-IR peaks at amide I region (1700 to 1600 $cm^{-1}$. C=O), amide II region (1600 to 1500 $cm^{-1}$, N-H), and amide III region (1300 to 1200 $cm^{-1}$, C-N) [15, 106]. As the hydrolysis time increased, it was found that β-sheet peaks at 1628, 1533, and 1265 $cm^{-1}$ shifted to corresponding random coil peaks at 1655, 1540, and 1235 $cm^{-1}$, respectively. Also, secondary structure content was calculated and compared from amide I region peak deconvolution using FT-IR spectra (**Figure 11B**). As expected, the β-sheet structure content increased with the $M_n$ of SF increment while the random coil structure content decreased. This was confirmed by thioflavin T assay. As shown in **Figure 12**, fluorescence intensity increased

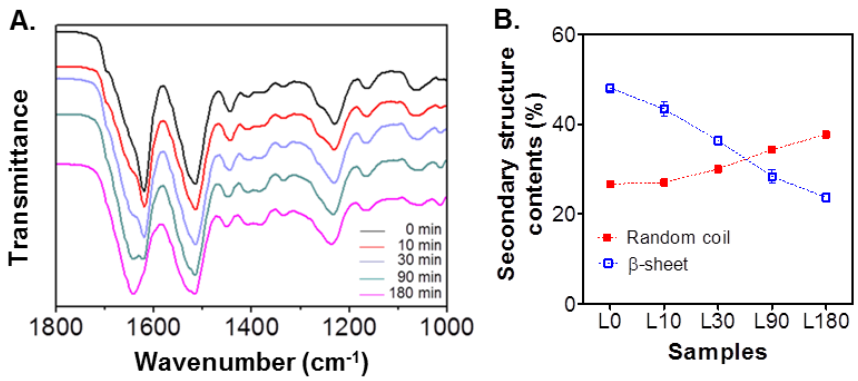


Figure 11. (A) FT-IR spectra and (B) secondary structure contents of freeze-dried SF hydrogels formed of different molecular weights of SF.

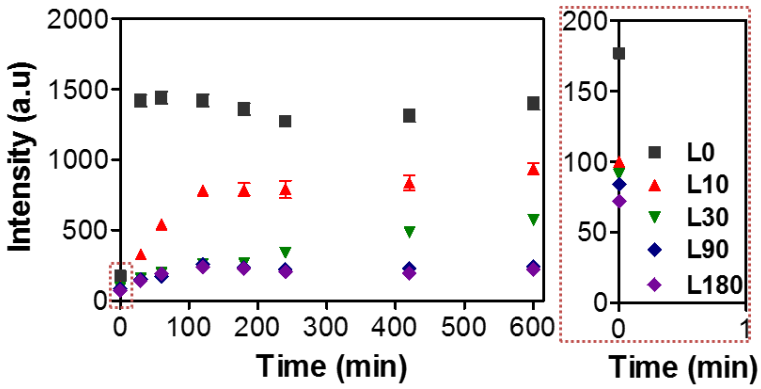


Figure 12. Thioflavin T fluorescence profiles of SF hydrogels formed of different molecular weights of SF, red box indicates the enlarged image of initial profiles at 0-time (mean ± SD, n = 3).

with the $M_n$ of SF increment and this trend was maintained for 600 min. This result is similar to that of FT-IR analysis. In short, the longer hydrolysis caused a significant damage of β-sheet participable segment, which finally lowers the β-sheet structure content of SF hydrogel (**Figure 11B and 12**). Consequently, the lowering the $M_n$ of SF did not efficiently form a hydrogel due to a lack of gel forming ability.

### 4.1.3. Physical properties of SF hydrogel

Gel fraction defines as the percentage of practical gel network participant polymer content of the hydrogel. On the other hand, swelling ratio indicates the capability of water absorption in hydrogel network structure. These parameters are frequently express the swelling characteristics of hydrogel material. **Figure 13A and 13B** present gel fraction and equilibrium mass swelling ratio of SF hydrogels, respectively. The hydrogel formed with intact SF (L0) showed about 98% gel fraction while the SF hydrogel of the lowest $M_n$ showed only 18%, indicating that most part of SF molecules of low $M_n$ did not participate in a gel formation. On the contrary, the swelling ratio increased as $M_n$ of SF decreased since the loose network of low $M_n$ SF had larger space to capture more water.

**Figure 14** shows equilibrium shear elastic modulus (G′) of SF hydrogels with different $M_n$ of SF. On the whole, the shear elastic modulus increased with $M_n$ of SF. However, the $M_n$ of SF that formed the stiffest SF hydrogel (L10, $G' \approx 16.7$ kPa) was not the intact SF but the hydrolyzed L10. It might be due to too rapid gelation of L0 during ultra-sonication, resulting in inhomogeneous network formation. It can be said that inhomogeneous network has more weak point than homogeneous one. Compared to 1-min ultra-sonicated L0 hydrogel, gel formation time of 3-min ultra-sonicated L0 was so fast and not sufficient to form the homogeneous gel structure. In addition, longer ultra-sonication treatment time increases the nucleation point

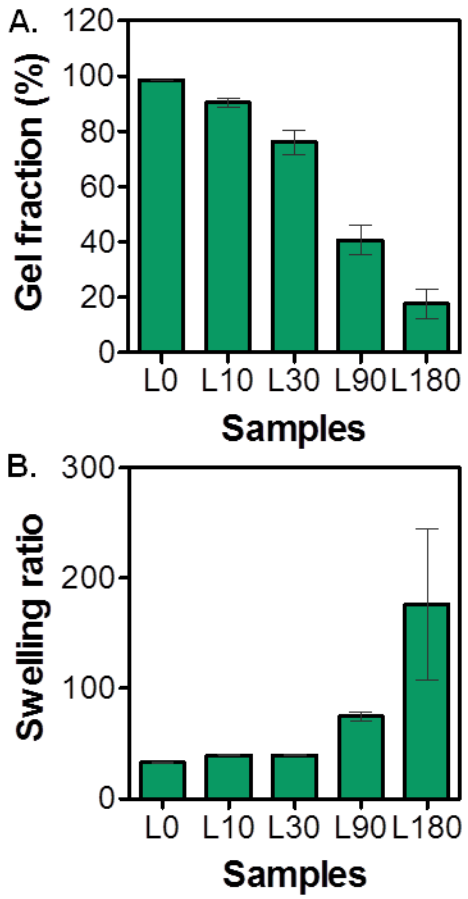


Figure 13. (A) Gel fraction and (B) equilibrium swelling ratio of SF hydrogels formed of different molecular weights of SF (mean ± SD, n = 3).

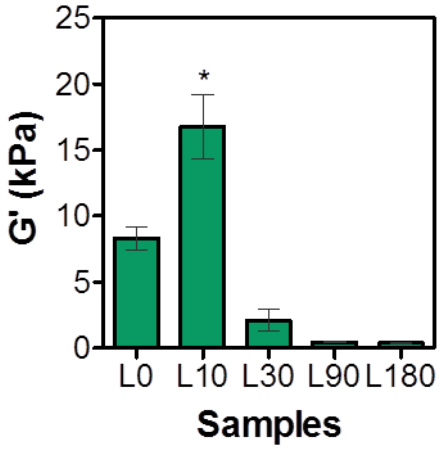


Figure 14. Equilibrium shear elastic modulus of SF hydrogels formed of different molecular weights of SF (mean ± SD, n = 3, *p < 0.01).

(seeding density) of SF aqueous solution [29], which can interrupt the growth of nucleation point. When the network growth of single nucleation point is restricted by another one, it has a small single domain network. This domain cannot be efficiently entangled with another network structure due to its small network size. Consequently, long ultra-sonication treatment lowers the G′ of SF hydrogel (**Figure 15**). In short, hydrolysis of SF critically affects the gel fraction, swelling ratio, and equilibrium shear elastic modulus of SF hydrogel.

Interestingly, it was found that the hydrolyzed SF solution and SF hydrogel exhibited quite different light transmittance in proportion to molecular weight of SF. Generally, SF hydrogel is opaque due to the formation of β-sheet crystalline structure [19]. The SF hydrogel fabricated from intact SF solution (L0) showed completely opaque, as shown in **Figure 16A**. Images of SF hydrogel also showed that its transparency gradually increased with an increment of hydrolysis time (L10 - L180). It seems that the crystallinity as well as crystal size may be crucial factors affecting the optical property of polymeric materials.

To compare the crystallinity of the hydrogels, a WAXD analysis was conducted (**Figure 17**). It has been known that the crystal structure of SF has specific [hkl] lattice plains, which attributed to [200] ($2\theta = 19.6°$), [201] ($2\theta = 23.3°$), and [100] ($2\theta = 8.7°$) [107, 108]. However, because of a wetted state, a main diffraction peak of [200] plain was shifted from 19.6° to 27° for the SF hydrogel [20]. Moreover, according to two-theta scan profiles of wide

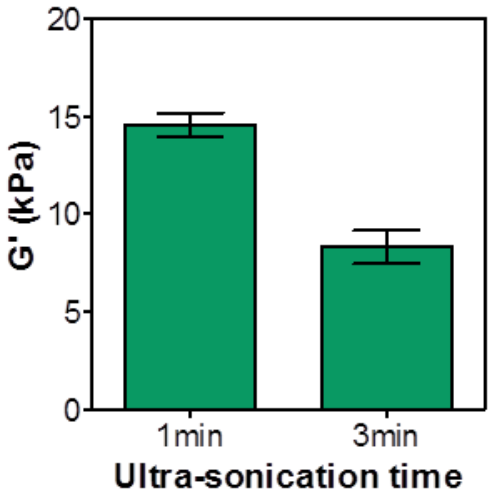


Figure 15. Equilibrium shear elastic modulus of SF hydrogels with different ultra-sonication time (mean ± SD, n = 3).

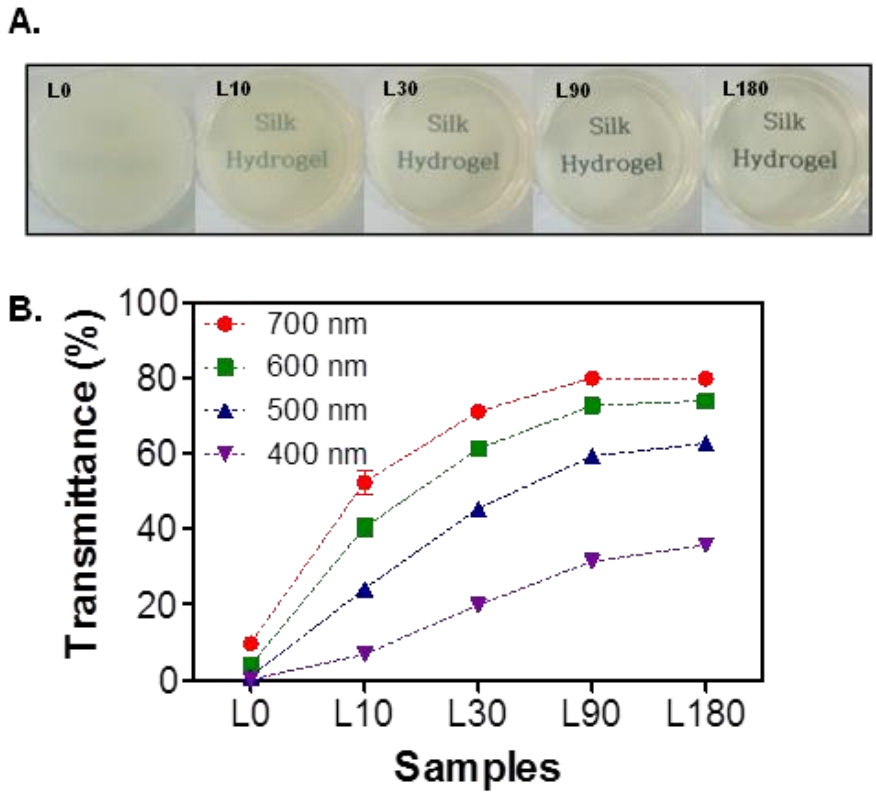


Figure 16. (A) Images of SF hydrogels formed of different molecular weights of SF. The bottom letters depicts transparency of each hydrogel. (B) Transmittance of SF hydrogels at different wavelength of visible light (mean ± SD, n = 3).

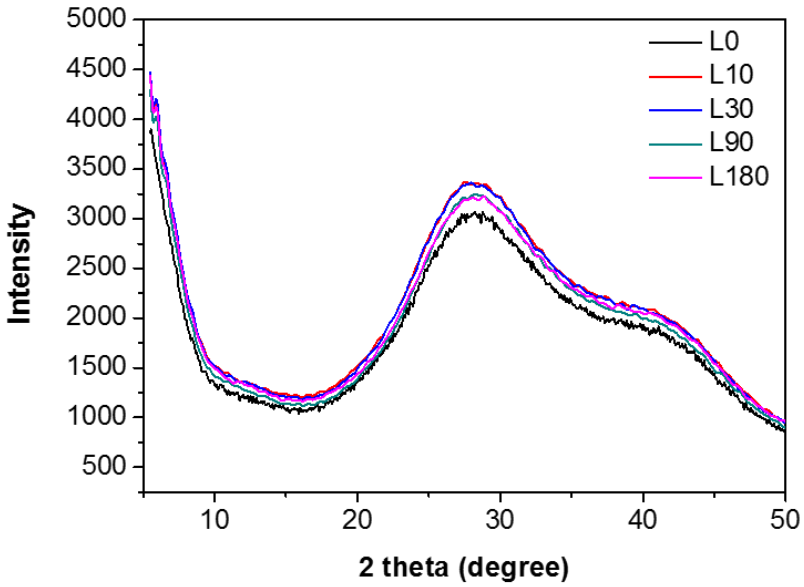


Figure 17. Two-theta scan profiles of WAXD analysis of SF hydrogels with different molecular weights of SF.

angle x-ray scattering (WAXS) pattern, noticeable difference in crystallinities of SF hydrogels could not be observed for different molecular weights of SF as shown in **Figure 17**. It might be due to a high water content (> 95%) in the hydrogel material. Therefore, the WAXD analysis is little useful to measure the crystallinity of SF hydrogel in addition to its precise crystal structure.

According to the conformational analysis of SF hydrogel measured by FT-IR spectroscopy and thioflavin T assay, the β-sheet content of SF decreased with an increment of hydrolysis time (**Figure 11 and 12**), indicating that the higher molecular weight of SF shows higher β-sheet crystalline content and higher crystallinity. Based on this result, it is speculated that variation of β-sheet crystalline content might influence the transparency of SF hydrogel. However, it is not the only factor determining the transparency of hydrogel because the hydrogel is basically a composite material of water phase and polymeric network. Therefore, the hydrogel can be opaque even if the polymeric phase is completely amorphous.

To quantitatively evaluate the optical property of SF hydrogels, the transmittance in the visible light wavelength range (400-700 nm) was measured using a spectrophotometer. **Figure 16B** shows the transmittance of SF hydrogel formed with different molecular weights of SF. The transmittance increased as the $M_n$ of SF decreased at all wavelengths while L0 showed less than 10% transmittance. Interestingly, an increment of transmittance with a

decrease of $M_n$ was much higher at a longer wavelength compared with a shorter one. Although L180 exhibited about 80% transmittance at 700 nm, the transmittance at 400 nm was lower than 40%. It can be noted that such different transmittances of SF hydrogels are closely related to a structural cluster which forms physical network structure of polymer chains [109]. When the cluster size is larger than visible light wavelength range (400-700 nm), visible light is scattered in hydrogel network structure. Herein, the transparency of SF hydrogel could increase when the cluster size became smaller than visible light wavelength range, indicating the shorter SF chains (i.e., lower $M_n$) make smaller clusters. Therefore, it is speculated that the average cluster size of transparent SF hydrogel would be mostly smaller than 400 nm (**Figure 16B**). Gap distance of clusters also affects the transparency of hydrogel. Regardless of cluster size, visible light can be scattered when the gap distance is smaller than visible light range. Exact gap distance of clusters is hard to be measured. However, it is estimated that average cluster gap distance of hydrolyzed SF hydrogels might be larger than visible light wavelength range.

### 4.1.4. Microstructure of SF hydrogel

To analyze microstructure of SF hydrogel, SAXS method was conducted. The SAXS analysis is known as a very powerful method for examining a long range structural order of polymer materials. **Figure 18A** shows SAXS curves of SF hydrogels with different molecular weights of SF. For further structural analysis, the SAXS curves were converted into $I(q)$ at the low $q^2$ region (0.007-0.024) using Guinier equation (Eq. (9)). **Figure 18B** shows Guinier plot curves of the SF hydrogels. The radius of gyration ($R_g$) obtained via Guinier plotting generally represents the gyration of a polymer chain in solution [110, 111]. In case of hydrogel, $R_g$ indicates the size of the polymer-rich solid-like domains (PRSD) [110]. The $R_g$ of SF hydrogel was in the range of 9.5-12.6 nm and also tended to increase with the $M_n$ of SF increment (**Figure 18C**). S. Nagarkar *et al*. previously reported that aggregates of SF hydrogel were composed of thin strands with less than 15 nm size in length [18]. These values correspond to the size of PRSD of SF hydrogel, which was derived from Guinier equation in this study. Accordingly, it was hypothesized that this PRSD was a smallest basic structural unit in SF hydrogel.

The shape of aggregate also can be determined from the Kratky plot of SAXS scattering curve [112]. Generally, the Kratky plot for globular structure shows a clear peak whereas that of random coil structure exhibits a plateau, followed by a gradual increase with q. As shown in **Figure 18D**, sample L0 showed a typical shape of peak for the globular structure. On the contrary, the

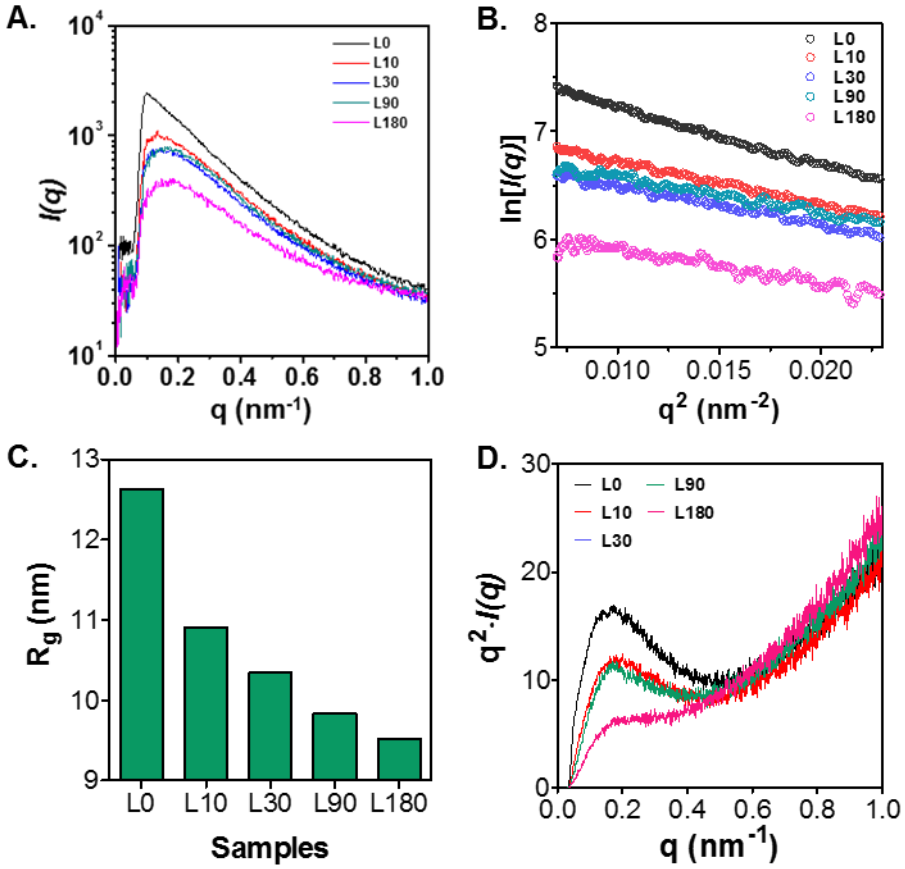


Figure 18. (A) SAXS curves, (B) Guinier plot curves, (C) Radius of gyration (derived from Guinier equation), and (D) Kratky plot curves of SF hydrogels with different molecular weights of SF.

shape of SF aggregate changed to that of random coil structure with the decrement of molecular weight of SF. It implies that hydrolysis affected the structural dissociation of SF aggregate, by changing from β-sheet to random coil conformation.

Based on the results in **Figure 16 and 18**, the microstructures of SF hydrogels, which are constituted of both un-hydrolyzed and hydrolyzed SF molecules, were depicted in **Figure 19**. In the un-hydrolyzed (opaque) SF hydrogel (L0 of the highest $M_n$), SF chains formed globular structured PRSD of 12-13 nm in diameter. After ultra-sonication treatment, those domains were agglomerated together to form single domain network. Then, these single domain networks were further grown to form hydrogel cluster, which can be considered as aggregated particle connected network or fibril entangled network (**Figure 20**) [18, 29]. The size of cluster was larger than visible light wavelength range (400-700 nm) and consequently, visible light could not penetrate the hydrogel network structure and scattered at the cluster of hydrogel. As a result, the hydrogel looks opaque. On the other hand, in the hydrolyzed (transparent) SF hydrogel (L180 of the lowest $M_n$), the fragmented SF chains formed relatively smaller random coil structured PRSD in the range of 9-10 nm and they built much smaller size of cluster than the visible light wavelength range. Consequently, highly hydrolyzed SF hydrogel did show a higher visible light transmittance (**Figure 16**). Improved transparency of the hydrolyzed SF hydrogel will be very useful for cell

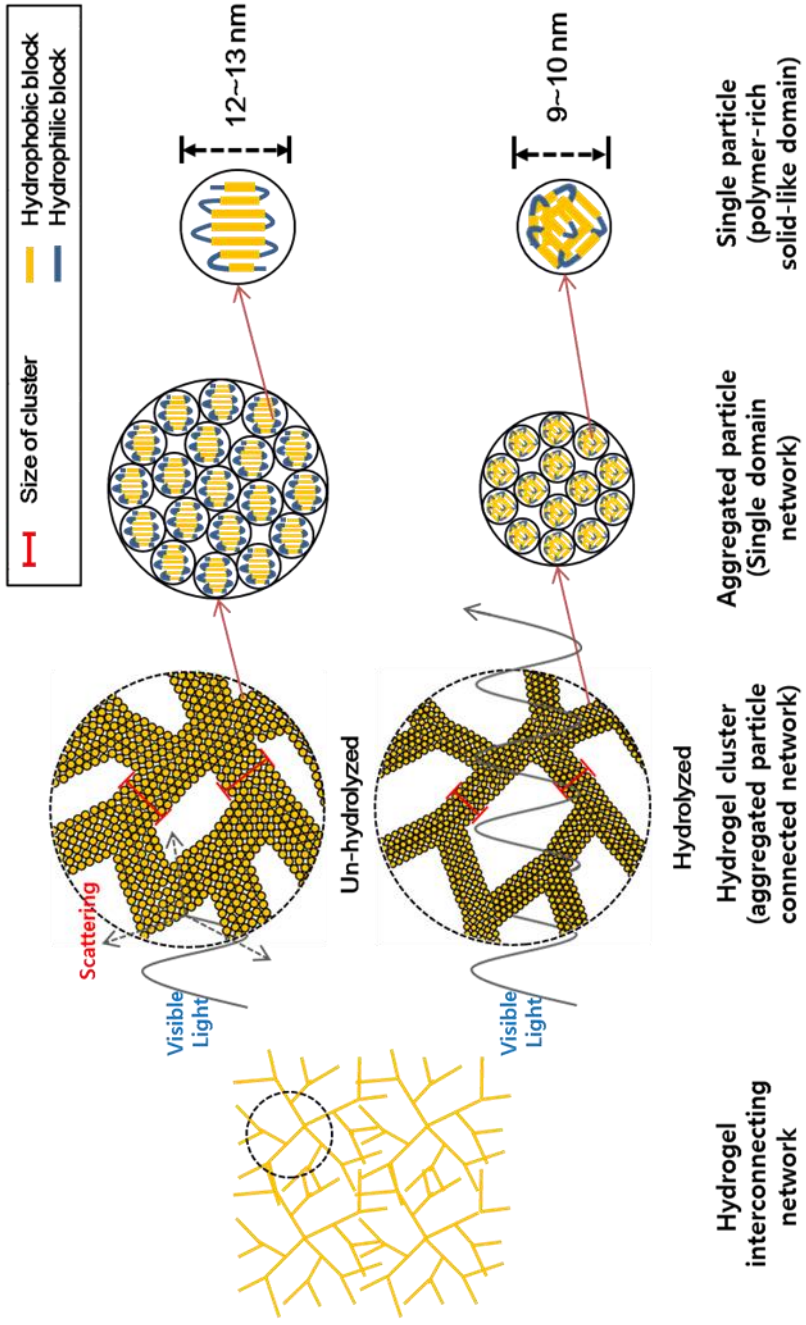


Figure 19. Schematic of microstructures of un-/180 min-hydrolyzed SF hydrogels.

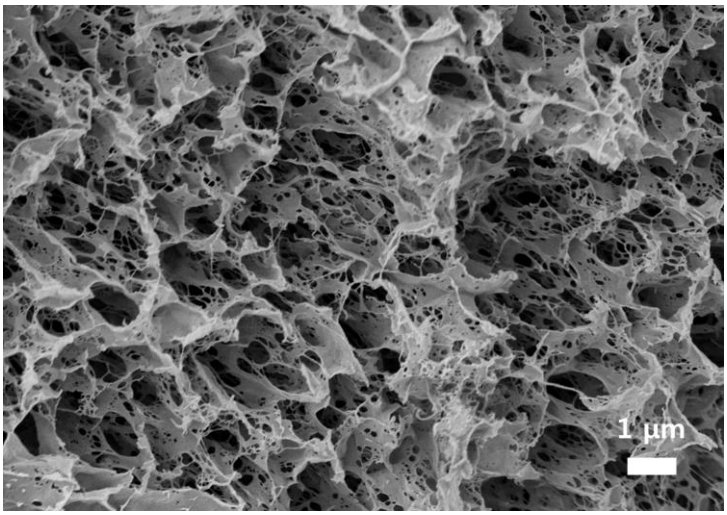


Figure 20. Cross-section image of freeze dried SF hydrogel (sample L0, un-hydrolyzed SF) observed by FE-SEM.

morphology observation as well as various biological assays. Most of all, the hydrolyis technique of SF (HAT method) can be applied to optical device development of silk-based biomaterials.

### 4.1.5. Cell adhesion behavior of SF hydrogel

The SF has been used for biomedical applications due to its excellent biocompatibility. Even though it has been reported that SF hydrogel has no cytotoxicity as well as a good cytocompatibility [20, 82, 83], cell adhesion behavior of physically crosslinked SF hydrogel was evaluated in this study. Here, hMSCs were cultured on the SF hydrogel for 24 hr. Phase-contrast images showed that the hMSCs were well attached and spread on relatively higher $M_n$ samples of SF hydrogels (i.e., L0, L10, and L30) while spherical shape of cells and less lived cells were observed on relatively lower $M_n$ sample of SF hydrogels (i.e., L90 and L180) (**Figure 21A**). Metabolic activity of hMSCs, cultured on the SF hydrogels of different molecular weights, was also examined (**Figure 21B**). The activity decreased significantly with the hydrolysis time of SF, which is corresponding to a decrease of the $M_n$ of SF. It can be said that the hMSCs cells prefers a stiff substrate (higher $M_n$ of SF hydrogel with higher shear elastic modulus) rather than a soft one (lower $M_n$ of SF hydrogel with lower shear elastic modulus).

**Figure 21C** shows confocal images of hMSCs on SF hydrogels after 24-hr post seeding, by depicting F-actin structure of the cells. In this confocal image, DAPI and rhodamine B can selectively stain the nucleus and F-actin of cells, respectively. It was found that F-actin was well developed on the whole cytoplasm of hMSCs on the SF hydrogel prepared using intact SF (L0, **Figure 21C**) while this observed at round boundary near cell membrane for the SF

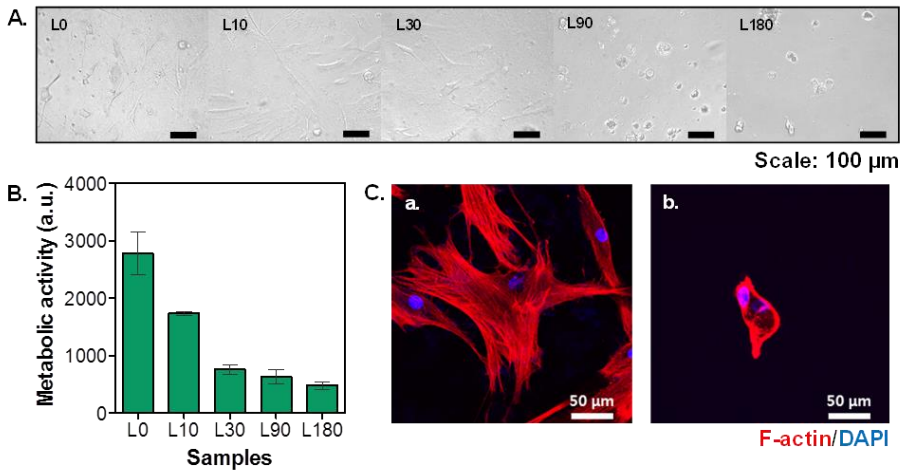


Figure 21. (A) Phase-contrast images of hMSC cultured on SF hydrogels of different hydrolysis times after 24-hour post-seeding (scale: 100 µm). (B) Metabolic activity of hMSC cultured on SF hydrogels of different molecular weights after 24-hour post-seeding (mean ± SD, n = 3). (C) Confocal images of hMSC on SF hydrogels after 24-hour post-seeding: (a) L0 and (b) L180 (F-actin: red, nucleus: blue).

hydrogel prepared with lowest $M_n$ of SF (L180, **Figure 21C**). It has been known that cell attachment and spreading are governed by stiffness of the matrix [113, 114]. A few hMSCs attached on the surface of soft L180 SF hydrogel with less spreading while many hMSCs remained and spread on the surface of stiffer SF hydrogel (L0) with well-developed actin cytoskeletons. It is concluded that different structural characteristics and gel properties of the SF hydrogels might affect the cell behavior, cell attachment, spreading, and proliferation.

## 4.2. CHEMICALLY PHOTO-CROSSLINKED SF HYDROGEL

### 4.2.1. Synthesis of SFMA

SF molecular chains innately prefer to be aggregated by making β-sheet crystalline structure in a rich region of repeated hydrophobic segments (Gly-Ala-Gly-Ala-Gla-X, X = Ser or Tyr). This structural property makes the SF molecules unstable in an aqueous solution and as a result, its hydrogel formation occurs at certain conditions. As mentioned before (**Figure 10**), the hydrogel formation, which is derived from the structural transition of SF, was retarded when the molecular weight of SF decreased. Therefore, by lowering the molecular weight of SF using HAT method (hydrolysis technique), chemically crosslinked SF hydrogel can be fabricated using photo-crosslinking method. Methacrylate (MA) functional groups were immobilized onto the hydrolyzed SF (synthesis of SFMA) and then photo-crosslinked SF hydrogel was prepared in this study.

The molecular weight of alkali-hydrolyzed SF used for the SFMA synthesis was measured by GFC (**Figure 22**). Intact SF had a sharp main peak at around 8.2 mL (~443 kDa), which is related to the molecular weight of SF heavy chains. As expected, when the hydrolysis time increased, the main peak gradually shifted to a lower molecular weight region at around 15.3 mL (~7 kDa). Using the HAT method for the hydrolysis of SF, various average molecular weights of SF could be successfully obtained in a range of 25 to 316 kDa. Then, the hydrolyzed SF was subsequently reacted with different

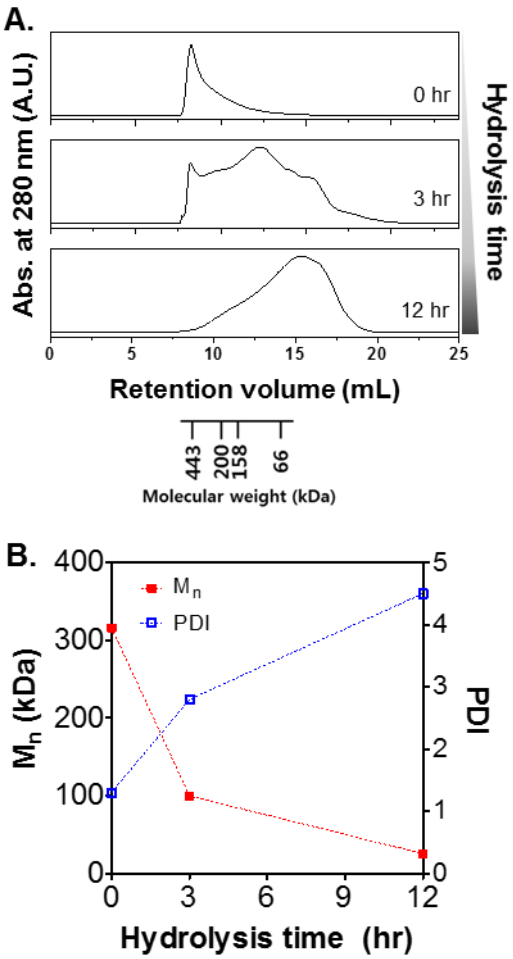


Figure 22. (A) Molecular weight distribution, (B) number average molecular weight ($M_n$), and polydispersity index (PDI) of the hydrolyzed SF prepared by HAT method.

concentration of IEM (in a range of 0.25 to 2.0 mmol/1 g SF) for the synthesis of SFMA. It was found that the solubility was significantly affected by a molecular weight of the SF and input IEM amount. In order to find out the optimum synthesis conditions of the SFMA, the solubility of SFMA in PBS was evaluated with respect to the two parameters, molecular weight of SF and input IEM amount (**Figure 23**). Regardless of input IEM amount, un-hydrolyzed SF was precipitated during dialysis. Such a precipitation is attributed to β-sheet structural transition of SF chains during solvent exchange from DMSO to $dH_2O$. On the other hand, the hydrolyzed SF samples ($M_n$: 25 to 210 kDa) maintained as a solution state during dialysis. This indicates that solution stability of SFMA is enhanced by a destruction of β-sheet domains of SF chains.

In addition to molecular weight of SF, input IEM amount also can affect the solubility of SFMA. **Figure 23** showed that its solubility decreased as an increment of the amount of hydrophobic IEM immobilized on SF. In case of 30 min hydrolyzed SF ($M_n$: 210 kDa), the solubility was dramatically reduced by input IEM amount. Even at a lower molecular weight region of SF ($M_n$: 25 to 100 kDa), the SFMA became insoluble when input IEM amount reached at 2.0 mmol per 1 g SF. As a result, it was found that only a 25 kDa and 100 kDa SF, which react with IEM to form the SFMA, could be completely dissolved in PBS in a specific range of input IEM amount (0.25 to 1.0 mmol/1 g SF). Consequently, the important point is that molecular weight decrease of SF can

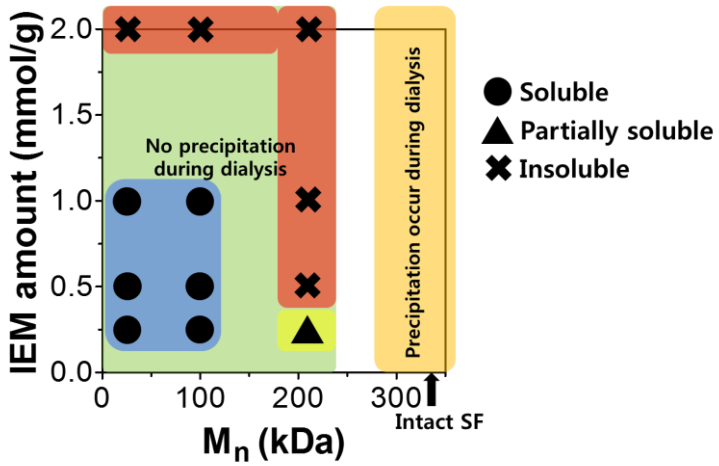


Figure 23. Solubility of SFMA in PBS with respect to a molecular weight of SF and input IEM amount.

enhance the stability of SF chains in aqueous solution. Furthermore, this enables a direct chemical modification of SF without precipitation during a reaction and dialysis process.

In this study, six SFMA hydrogel samples (sample ID: 25_0.25, 25_0.5, 25_1.0, 100_0.25, 100_0.5, and 100_1.0) were selected for the fabrication of SFMA hydrogels (photo-crosslinked SF hydrogels) (**Table 6**). Then, the effect of immobilized MA amount on SF and molecular weight of SF, were intensively studied on the structural characteristics and physical properties (including gel properties) of the SFMA hydrogels.

Table 6. Sample ID and preparation conditions of SFMA hydrogels.

| Sample ID | $M_n$ of SF (kDa) | Input IEM amount (mmol/g) |
|---|---|---|
| 25_0 | 25 | 0 |
| 25_0.25 | | 0.25 |
| 25_0.5 | | 0.5 |
| 25_1.0 | | 1.0 |
| 100_0 | 100 | 0 |
| 100_0.25 | | 0.25 |
| 100_0.5 | | 0.5 |
| 100_1.0 | | 1.0 |

### 4.2.2. $^{1}$H NMR analysis of SFMA

SF protein contains reactive functional moieties of hydroxyl (i.e., serine, tyrosine, and threonine), carboxyl (i.e., aspartic acid and glutamic acid), and amine (i.e., arginine and lysine) groups. Theoretically, 14.2 mol% of hydroxyl groups exists in SF while only 1.1 mol% and 0.6 mol% of carboxylic and amine groups, respectively, occupied the side group of SF residues [77]. Therefore, it is advantageous to target the hydroxyl groups of SF for introducing large amount of functional group into SF and also for obtaining high reaction yield and desirable properties. It was reported that isocyanate group can be reacted with both hydroxyl and amine groups of SS and SF under mild heating condition [38, 115]. In case of reaction between SF and IEM for the synthesis of SFMA, the reaction mechanism was proposed previously in **Figure 7**. Both hydroxyl and amine group of SF can be reacted with isocyanate group of IEM to introduce MA group onto SF. Therefore, in this study, $^{1}$H NMR analysis was performed for confirming the reaction and also for calculating an immobilized MA amount on SF and reaction yield of SFMA.

**Figure 24A** shows $^{1}$H NMR spectra of 12 hr hydrolyzed SF (25_0) and SFMA (25_1.0). In case of un-modified SF ($M_n$: 25 kDa), typical multiple peaks of SF protein were observed, which are attributed to Gly (α: 3.94), Ala (α: 4.29-4.45, β: 1.1-1.5), Ser (α: 4.29-4.45, β: 3.94), Tyr (4H: 6.5-7.5, α: 4.6, β: 2.65-3.05), and Val (γ: 0.9) residues in SF heavy chain [116, 117]. When

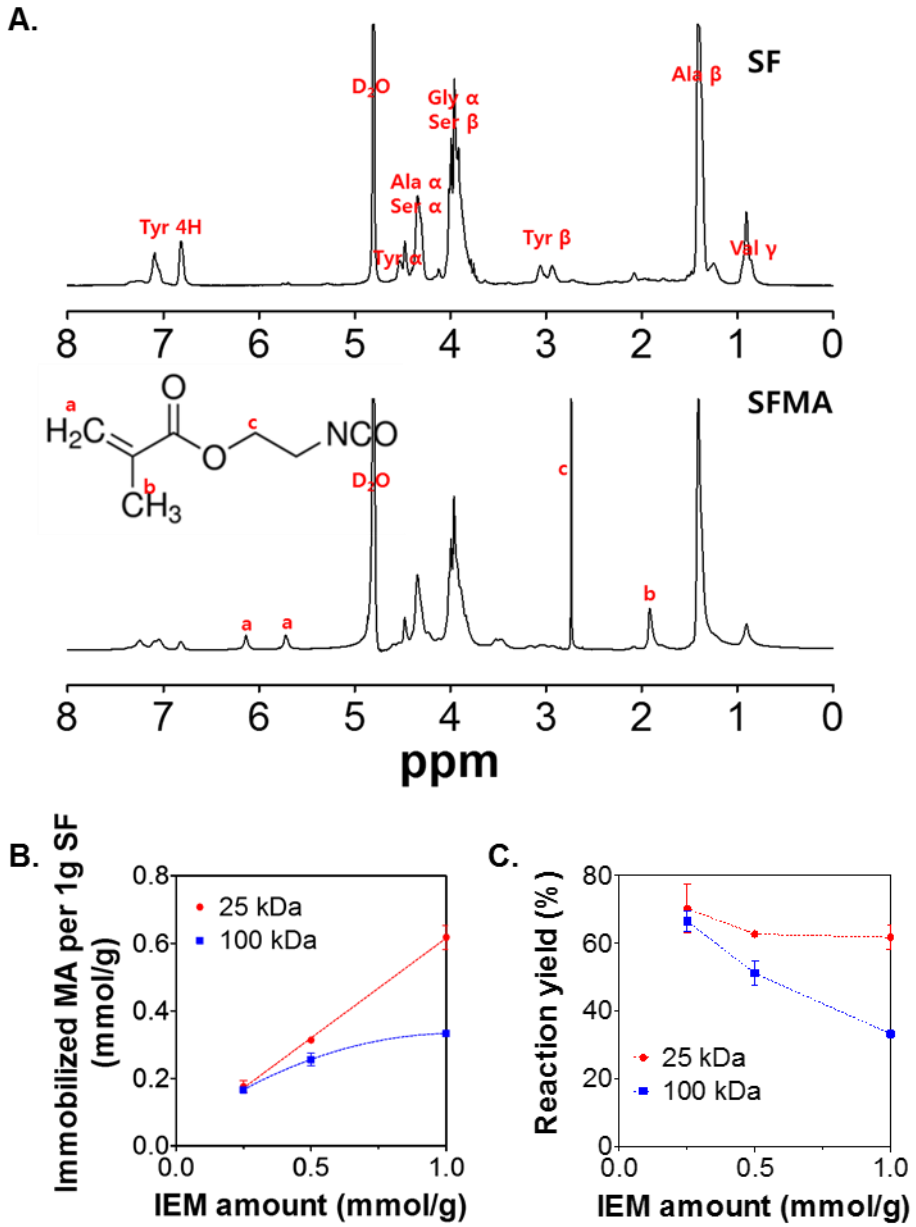


Figure 24. (A) 600 MHz $^{1}$H NMR spectra of 12 hr hydrolyzed SF (25_0) and SFMA (25_1.0) ($D_2O$ was used as a solvent) (B) Immobilized amount of methacrylate group (MA) on SF and (C) reaction yield of SFMA (n = 3, mean ± SD).

the IEM introduced to SF chains, double peaks, attributed to $CH_2$ (a: vinyl double bond) of IEM appeared at 6.13 and 5.72 ppm in $^1$H NMR spectra of SFMA. Also, $CH_3$ (b: methacrylate methyl group) and $CH_2$ (c: ethyl group) peaks of IEM were located at 1.75 and 1.91 ppm, respectively [118, 119]. The reaction between IEM and SF was not verified but it confirmed that the IEM was well introduced and possibly immobilized onto SF.

In order to calculate the immobilized MA amount on SF and reaction yield of SFMA using Eq. (1), (2), and (3) (section 3.4.2.), analysis of amino acid composition and $^1$H NMR were performed. As a result of amino acid analysis, 5.19 and 5.71 mol% of Tyr were contained in 3 hr and 12 hr hydrolyzed SF, which is corresponding to 100 kDa and 25 kDa SF, respectively (**Table 7**). Also, the areas of specific $^1$H NMR peaks were measured using $^1$H NMR spectra of SF and SFMA for the calculation (**Figure 25**).

In **Figure 24B and 24C**, immobilized MA per 1g of SF and reaction yield of SFMA were plotted against input IEM amount for different molecular weight of SF, 25 kDa and 100 kDa. It was found that immobilized MA amount on 25 kDa SF linearly increased with an increment of input IEM amount. On the contrary, immobilized MA amount on 100 kDa SF was relatively lower than that on 25 kDa SF. This is the reason why reaction yield of SFMA, prepared with 100 kDa SF, decreased to about 33%.

On the other hand, SFMA, prepared with 25 kDa SF, maintained the reaction

Table 7. Amino acid composition (mol%) of un-hydrolyzed (pristine SF) and hydrolyzed SF.

| **Amino acids** | **Pristine SF (mol%)** | **100 kDa SF (mol%)** | **25 kDa SF (mol%)** |
|---|---|---|---|
| Alanine | 29.46 | 31.12 | 31.54 |
| Arginine | 0.64 | 0.46 | 0.55 |
| Aspartic acid | 1.66 | 1.73 | 2.03 |
| Cysteine | Not detected | Not detected | Not detected |
| Glutamic acid | 1.10 | 1.33 | 1.62 |
| Glycine | 44.09 | 45.90 | 44.56 |
| Histidine | 0.35 | 0.15 | 0.21 |
| Isoleucine | 0.76 | 0.41 | 1.06 |
| Leucine | 0.61 | 0.44 | 0.87 |
| Lysine | 0.38 | 0.03 | 0.09 |
| Methionine | Not detected | Not detected | Not detected |
| Phenylalanine | 0.82 | 0.67 | 1.05 |
| Proline | 0.53 | 0 | 0 |
| Serine | 11.31 | 10.21 | 7.90 |
| Threonine | 1.10 | 0.61 | 0.59 |
| Tryptophan | Not detected | Not detected | Not detected |
| Tyrosine | 5.15 | **5.19** | **5.71** |
| Valine | 2.04 | 1.78 | 2.22 |
| Total | 100 | 100 | 100 |

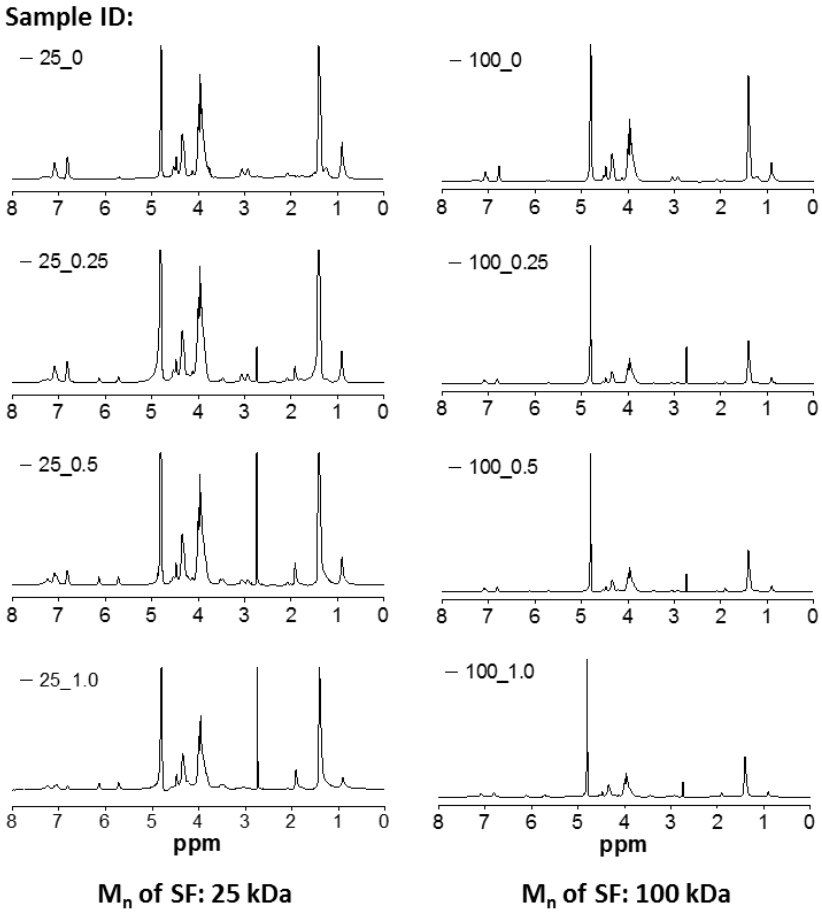


Figure 25. 600 MHz $^{1}$H NMR spectra of SF and SFMA prepared with various molecular weight of SF ($D_2O$ was used as a solvent).

yield to more than 60% even though the input IEM amount was increased (**Figure 24C**). The difference might be due to the structural characteristic of SF in organic solvent, DMSO. SF molecules mainly consist of hydrophobic segment with little amount of hydrophilic segment and they show the micellar structure in solution state due to their amphiphilic property [120, 121]. Hydrophobic segment of 100 kDa SF is relatively well preserved compared to 25 kDa SF and consequently, its hydrophobic part efficiently disturbs the contact of IEM with hydrophilic part of SF (reactive site of SF) more than that of 25 kDa SF. As a result, more IEM could be immobilized on the 25 kDa SF at a same IEM concentration with a high reaction yield.

### 4.2.3. Gelation behavior of SFMA hydrogel

In order to compare physical properties of SFMA hydrogels with respect to immobilized MA amount on SF and molecular weight of SF, optimum concentration of synthesized SFMA for gel formation should be fixed. As shown in **Figure 26**, general trend was observed that minimum (critical) gel forming concentration decreased with an increment of immobilized MA amount on SF. This is due to that the gel formation is preferable at MA-rich condition. **Figure 26** also showed that all SFMA hydrogels could be formed above 12 wt% concentration and consequently the optimum concentration condition was selected as 12.5 wt% of SFMA for further studies.

As mentioned previously (**Figure 8)**, photo-crosslinking reaction of SFMA was conducted for fabrication of SFMA hydrogel using a photo-initiator, LAP, under UV irradiation condition. **Figure 27** shows in situ photo-rheometry results for SFMA precursor solutions of different molecular weight of SF and input IEM amount. It elucidates the results of shear moduli (G′ and G″) variations before and after UV irradiation. It was found that the reaction was completed within 1 min after UV irradiation. Consequently, gel points of SFMA hydrogels, which were formed of different immobilized MA amount and molecular weight of SF, were measured (**Figure 28**). It demonstrated that the immobilized MA amount on SF mainly affects the gel formation of SFMA compared to the effect of molecular weight of SF. Especially, highly immobilized SFMA (Sample ID: 25_1.0) showed a shortest gel point about

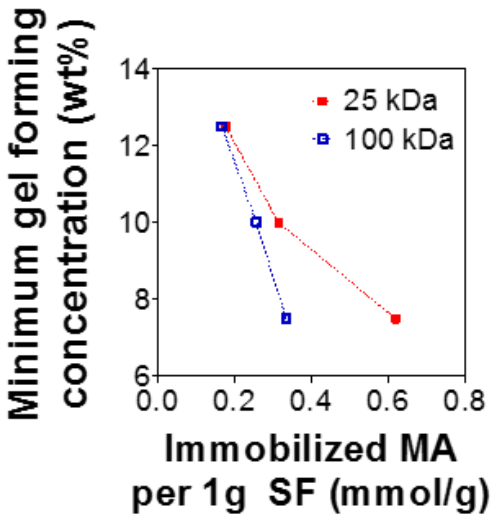


Figure 26. Minimum gel forming concentration of SFMA formed of different immobilized MA amount and molecular weight of SF.

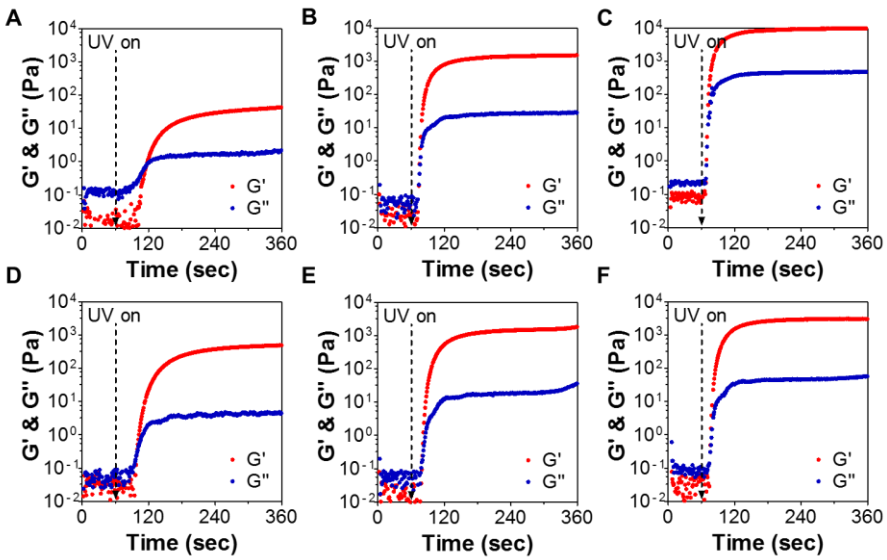


Figure 27. In situ photo-rheometry results of SFMA precursor solutions. (A) 25_0.25, (B) 25_0.5, (C) 25_1.0, (D) 100_0.25, (E) 100_0.5, and (F) 100_1.0. UV light source was turned on at 60 s after the onset of measurements (same concentration: 12.5 wt%).

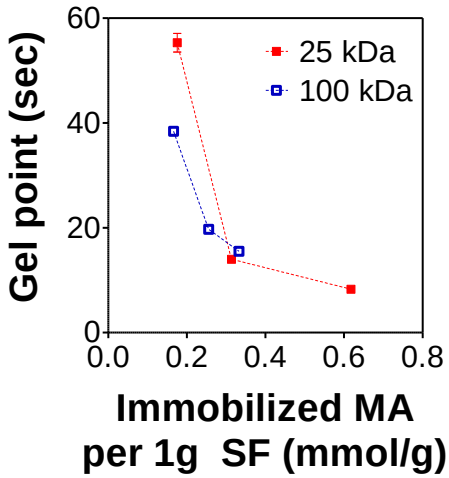


Figure 28. Gel points of SFMA hydrogels formed of different immobilized MA amount and molecular weight of SF (same concentration: 12.5 wt%) (n = 3, mean ± SD).

8.2 sec, indicating that the gel formation of SFMA can be facilitated with the increment of immobilized MA amount on SF.

### 4.2.4. Physical properties of SFMA hydrogel

As same as gel forming ability, two important parameters, such as immobilized amount of MA group onto SF and molecular weight of SF, might also affect physical properties of the photo-crosslinked SF hydrogels (SFMA hydrogels). Therefore, such as gel properties, optical property, thixotropic property, and resilience were examined and compared.

#### 4.2.4.1. Gel properties

**Figure 29** shows gel fraction and swelling ratio of the SFMA hydrogels formed of different immobilized MA amount and molecular weight of SF. Gel fraction increased with an increment of immobilized MA amount (**Figure 29A**). Higher gel fraction (> 88%) was obtained when MA immobilized amount on SF was more than 0.25 mmol per 1 g of SF. On the other hand, half of 25_0.25 SFMA sample could not participate in gel formation. Contrary to the result of gel fraction, swelling ratio of the SFMA hydrogels decreased with an increment of immobilized MA amount, regardless of molecular weight difference (**Figure 29B**). The hydrogels showed the swelling ratio in a range of 7.6 to 21.8.

Equilibrium shear elastic modulus (G′) of the SFMA hydrogels was also measured and compared. As shown in **Figure 30**, G′ of the hydrogels increased with an increment of immobilized MA amount. Even though the concentration of the hydrogel was same (12.5 wt%), it had a wide range of G′

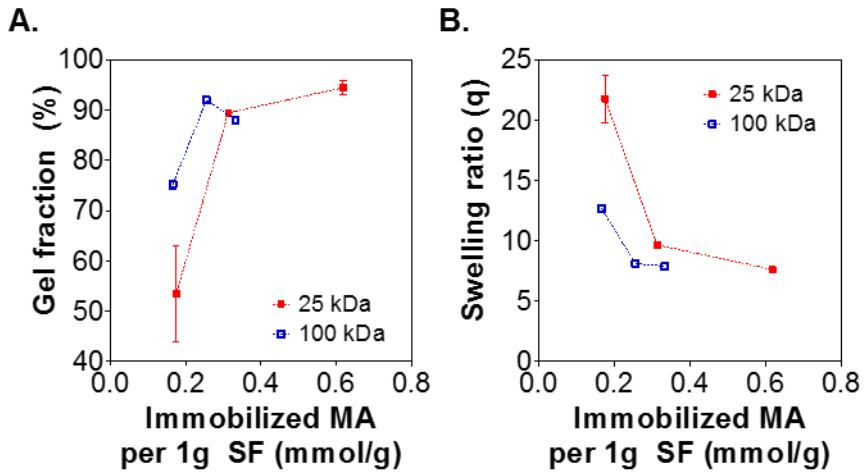


Figure 29. (A) Gel fraction and (B) swelling ratio of SFMA hydrogels formed of different immobilized MA amount and molecular weight of SF (same concentration: 12.5 wt%) (n = 3, mean ± SD).

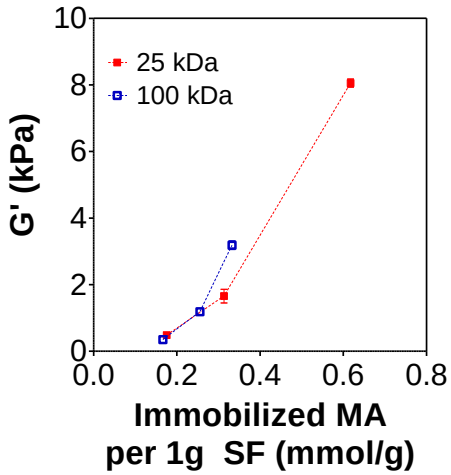


Figure 30. Equilibrium shear elastic modulus (G′) of SFMA hydrogels formed of different immobilized MA amount and molecular weight of SF (same concentration: 12.5 wt%) (n = 3, mean ± SD).

values of 3 to 80 kPa. In short, the immobilized MA amount on SF might more significantly affect the gel properties of SFMA hydrogel than molecular weight of SF. However, in case of swelling ratio, the molecular weight difference (25 kDa vs 100 kDa) is a major factor to affect the gel property. This is because a chain length of 100 kDa SF is relatively longer than that of 25 kDa and may hinder the swelling of whole network structure.

In this study, the concentration of SFMA hydrogel was fixed as 12.5 wt%. However, the concentration of hydrogel mostly influences its physical properties in general. It was found that when the concentration of hydrogel increased, gel fraction and G′ of SFMA hydrogels were increased while swelling ratio decreased (**Figure 31, 32, and 33**). The variation in these gel properties was higher for 25 kDa SFMA hydrogel. It is because difference of immobilized MA amount on SF among the samples was larger in 25 kDa SFMA hydrogels than 100 kDa SFMA samples.

In an application point of view, it is said that physical properties (including gel properties) of SFMA hydrogel can be manipulated via controlling the fabrication parameters, such as the immobilized MA amount on SF, molecular weight of SF, and concentration of SFMA precursor solution.

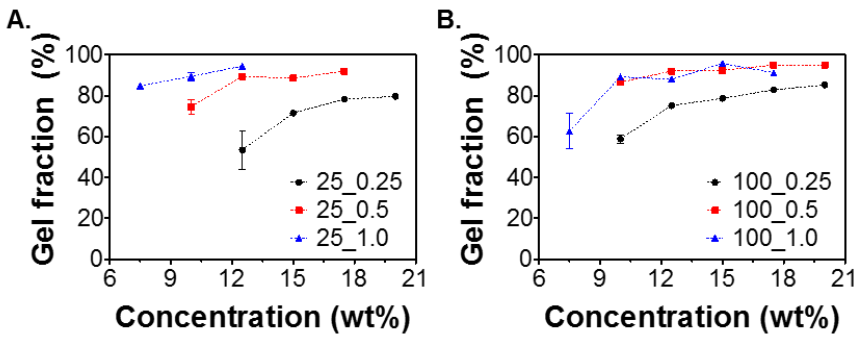


Figure 31. Gel fraction of SFMA hydrogels with various concentrations. (A) 25 kDa SF, (B) 100 kDa SF (n = 3, mean ± SD).

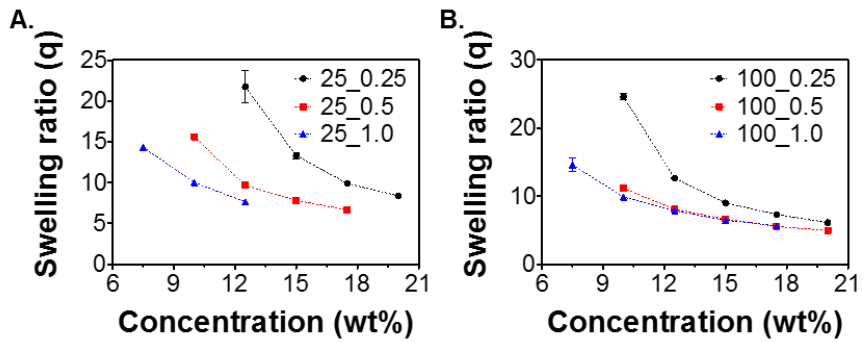


Figure 32. Swelling ratio of SFMA hydrogels with various concentrations. (A) 25 kDa SF, (B) 100 kDa SF (n = 3, mean ± SD).

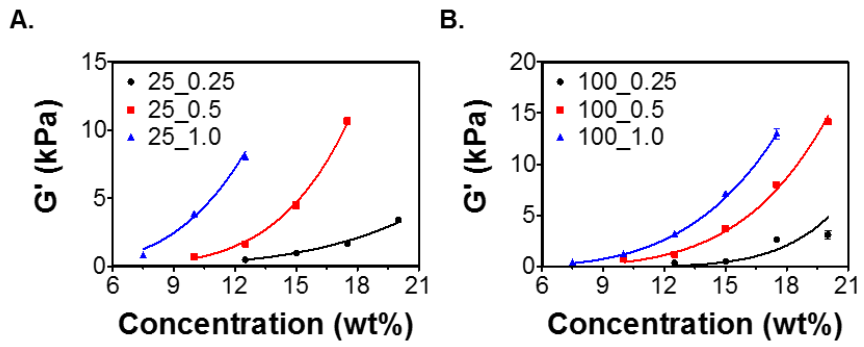


Figure 33. Equilibrium shear elastic modulus (G') of SFMA hydrogels with various concentrations. (A) 25 kDa SF, (B) 100 kDa SF (n = 3, mean ± SD).

#### 4.2.4.2. Transparency of SFMA hydrogel

In order to find out optical property of the hydrogel, transmittance in the visible light wavelength range (400-800 nm) of SFMA hydrogels was analyzed by using a spectrophotometer. As shown in **Figure 34**, the transmittance at all wavelengths decreased with an increment of immobilized MA amount on SF and molecular weight of SF. It implies that increased photo-crosslinking points of SFMA hydrogel network act as scattering points for a visible light. Moreover, the longer the chain length of SF (100 kDa SF), the lower the transparency of SFMA hydrogel, indicating that SF chain length (molecular weight of SF) also affects the visible light scattering and its effect is clearly observed for a longer chain length. When the SFMA hydrogel is used as an optical materials, the transparency is an important property and this can be also controlled by the immobilized MA amount on SF as well as molecular weight of SF in the hydrogel.

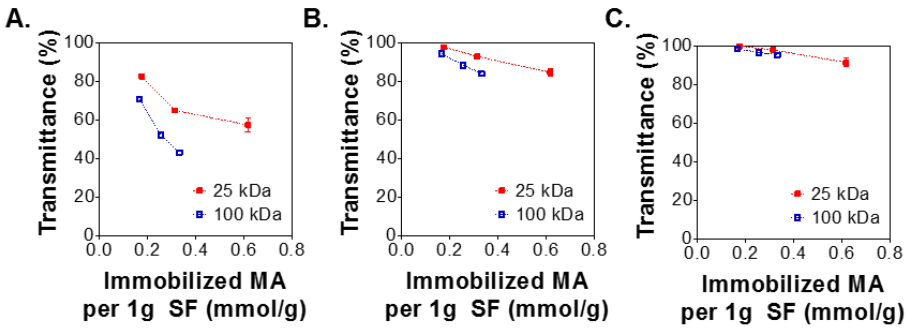


Figure 34. Transmittance of SFMA hydrogels formed of different immobilized MA amount and molecular weight of SF at (A) 400 nm, (B) 600 nm, and (C) 800 nm of visible light wavelength (same concentration: 12.5 wt%) (n = 3, mean ± SD).

### 4.2.4.3. Thixotropic property of SFMA hydrogel

Thixotropic property of SFMA hydrogel was examined when a certain level of stress was applied to the hydrogel. Thixotropic property is a time-dependent shear thinning property. When sufficient stress is applied to gel (viscous) material, it can flow temporarily but returns to a gel state after removing of applying stress. This behavior is essential in an application of injectable hydrogel material. **Figure 35** shows a fluidic behavior ($G'' > G'$) when the stress applied to the hydrogel with higher than 300 Pa. It was also shown that $G'$ of the 25_1.0 hydrogel was sufficient for withstanding 300 Pa of stress, exhibiting a crossover point of $G'$ and $G''$ at 950 Pa (**Figure 36**). It seems that crossover point of stress increases with an increment of equilibrium shear elastic modulus of the hydrogel. In case of 25_0.25 hydrogel sample, it showed a thixotropic property at very low stress point (0.34 Pa). It is because gel fraction and equilibrium shear elastic modulus of the 25_0.25 hydrogel is too low compared to other SFMA hydrogels. Interestingly, 25_0.5 SFMA hydrogel showed a reversible thixotropic property (**Figure 37**), implying that physical crosslinking exists in a hydrogel network structure. Therefore, it is suggested that this thixotropic behavior of SFMA hydrogels can be used as an injectable material.

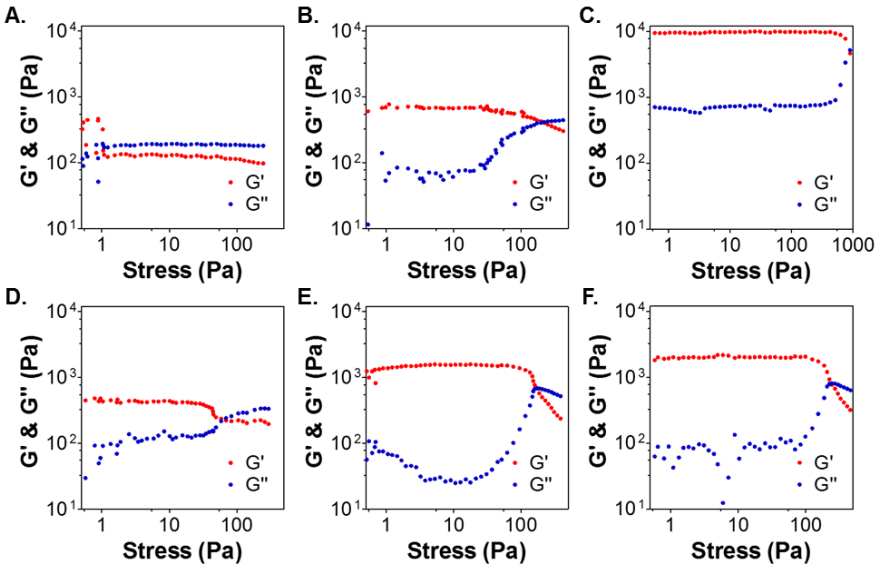


Figure 35. G′ and G″ variation of SFMA hydrogels formed of different immobilized MA amount and molecular weight of SF at stress-sweep oscillatory mode for thixotropic property analysis (same concentration: 12.5 wt%).

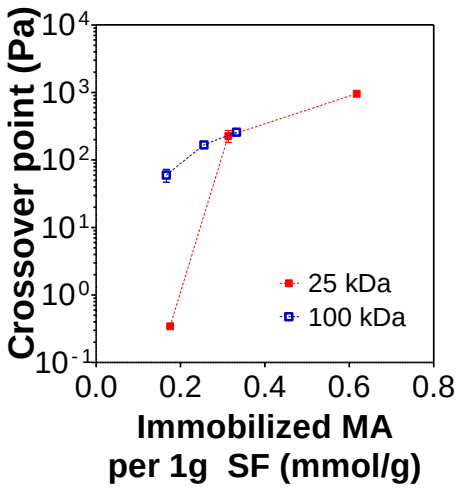


Figure 36. Crossover point (G′ = G″) of SFMA hydrogels formed of different immobilized MA amount and molecular weight of SF at stress-sweep oscillatory mode for thixotropic property analysis (same concentration: 12.5 wt%).

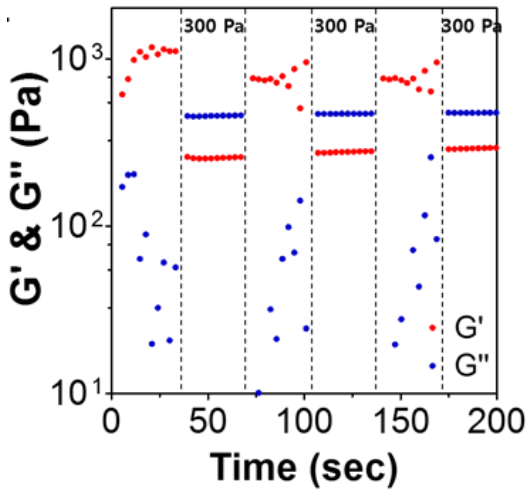


Figure 37. G′ and G″ variation of SFMA hydrogel (Sample ID: 25_0.5) when stress was applied (300 Pa) and released (0.1 Pa), alternatively.

### 4.2.4.4. Resilience of SFMA hydrogel

Resilience of SFMA hydrogels was evaluated by compressive cyclic test. **Figure 38** shows cyclic compression curves of the hydrogels formed of different immobilized MA amount on SF and molecular weight of SF. 50 times of cyclic compressive test were performed when 20% of compressive strain was applied. All the SFMA hydrogels showed that initial compressive stress increased with an increment of immobilized MA amount, except 100_1.0 SFMA hydrogel sample. And the compressive stress mostly recovered to original stress value even after 50 times cycling.

In order to compare compressive property of the SFMA hydrogel (chemically crosslinked SF hydrogel) with that of physically crosslinked SF hydrogel, 3 times of cyclic compressive test was performed and S-S curves results are shown in **Figure 39**. For an accurate comparison, 100_0.5 SFMA hydrogel sample, which has a same G′ condition of physically crosslinked SF hydrogel, was chosen. When the strain was applied, physically crosslinked SF hydrogel was highly damaged at just one cycle of compression and after several cycling, it deformed permanently and lost its original shape (**Figure 39A**). This indicates that the physically crosslinked SF hydrogel has a poor compressive property.

On the other hand, chemically crosslinked SF hydrogel showed similar S-S curves after 3 times repeating compression without any hysteresis (no energy loss) (**Figure 39B**). Moreover, as shown in **Figure 38**, compressive stress at

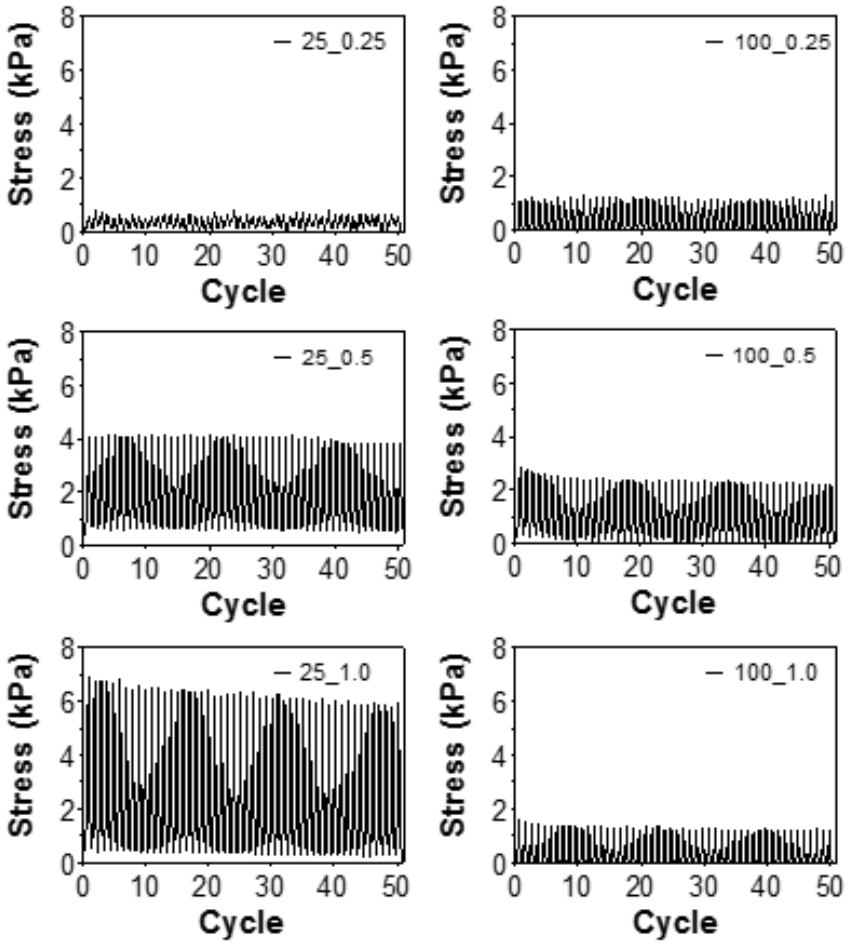


Figure 38. Cyclic compression curves of SFMA hydrogels formed of different immobilized MA amount of SF and molecular weight of SF from 50 times of cyclic compressive test when 20% of compressive strain was applied (same G′ ~ 1.3 kPa).

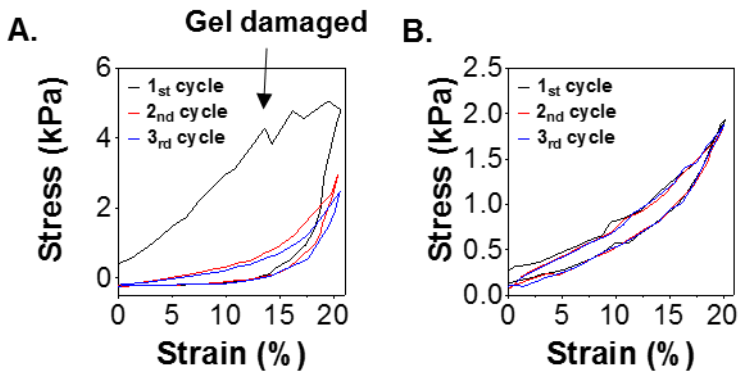


Figure 39. S-S curve results from 3 times of cyclic compressive test (A) physically crosslinked and (B) chemically crosslinked (100_0.5 SFMA hydrogel sample) SF hydrogels.

20% strain of this SFMA hydrogel was mostly recovered after 50 times of cyclic compression. Even when 50% of compressive strain was applied to this hydrogel, a deformed shape recovered immediately without crack formation and maintained its original shape permanently (**Figure 40**). Therefore, it can be said that mechanical properties of chemically crosslinked SF hydrogel is superior to physically crosslinked one. Specially, the resilience of SF hydrogel can be markedly enhanced by chemical covalent bond formation via photo-crosslinking. It is also notified that somewhat deficient mechanical property of the SFMA hydrogel, which was derived from the use of hydrolyzed SF (low molecular weight of SF), could be compensated through the formation of chemically crosslinked network structure.


Figure 40. Before and after images of chemically crosslinked SF hydrogel (100_0.5 SFMA hydrogel sample) when 50% of compressive strain was applied.

### 4.2.4.5. Degradation behavior of SFMA hydrogel

Degradation behavior of SFMA hydrogels was analyzed by tracking G′ variation using rheometry. **Figure 41** shows the changes of shear elastic modulus (G′) and degradation rate constant (k′) of the hydrogels formed of different immobilized MA amount on SF and molecular weight of SF. IEM, which was used for the synthesis of SFMA, has an ester bond in backbone chain that it is vulnerable to hydrolytic degradation. In this reason, the hydrogels with a low immobilized MA amount (25_0.25 and 100_0.25 SFMA hydrogel samples) were fully degraded within 2 days. On the other hand, it maintained an original shape when MA immobilized amount on SF was higher than 0.33 mmol per 1 g of SF even though the G′ gradually decreased in PBS (**Figure 41A and 41B**).

Regardless of immobilized MA amount on SF, all of the hydrogels showed a first order rate of degradation for first 7 days. Therefore, in this period, degradation rate constant (k') was derived using Eq. (6) (section 3.4.4.3.). As shown in **Figure 41C**, the k' decreased with an increment of immobilized MA amount. Especially, it showed high k' when immobilized MA was less than 0.18 mmol per 1 g of SF. This indicates that highly crosslinked SFMA hydrogel has higher structural stability in aqueous environment. As shown in **Figure 41A and 41B**, after rapid degradation, G′ of the hydrogels (e.g., 25_0.5, 25_1.0, and 100_1.0 SFMA hydrogel samples) reached a plateau for a while, indicating that another crosslinking bonding also exists in a hydrogel

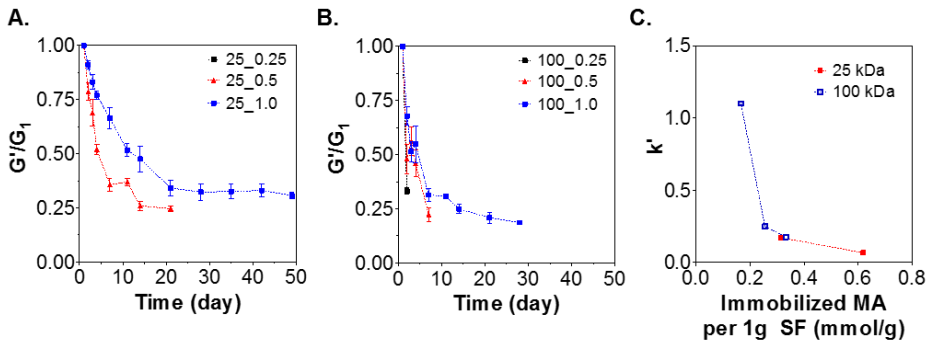


Figure 41. (A) (B) Changes of shear elastic modulus (G′) and (C) degradation rate constant (k′) of SFMA hydrogels formed of different immobilized MA amount on SF and molecular weight of SF (n = 3, mean ± SD). All the hydrogels were incubated in PBS at 37℃ for 48 days.

network. Interestingly, 25_1.0 SFMA hydrogel showed a stable G′ plateau and it maintained an original form for more than 48 days.

### 4.2.5. Microstructure of SFMA hydrogel

Microstructure of SFMA hydrogel was examined using SAXS method and **Figure 42A** shows SAXS curves of the hydrogels formed of different immobilized MA amount and molecular weight of SF. Similar shape of curves was obtained among the hydrogel samples. For a detailed analysis, the SAXS curves were conducted using Kratky plot, which is useful for analyzing a structural shape of aggregates in hydrogel network. In case of SFMA hydrogels prepared with 25 kDa SF, specific peak appeared at around 0.22 $nm^{-1}$ and it became narrower with an increment of immobilized MA amount (**Figure 42B**). On the contrary, SFMA hydrogels prepared with 100 kDa SF showed a shoulder peak at same q position (**Figure 42C**). Structural difference of the hydrogels is not clearly elucidated from Kratky analysis but the immobilized MA amount on SF might affect their microstructures. Specially, its effect on a structural change is more prominent in the case of lower molecular weight of SF (25 kDa SF). The peak in Kratky plot is known that a shape of aggregates in hydrogel network structure is a globule [111, 112]. Therefore, globular structure seems be preferably formed in SFMA hydrogel of 25 kDa SF rather than that of 100 kDa SF.

CD analysis can be frequently used for determining a secondary structure of proteins. In case of SF protein, a random coil, β-sheet, and α-helix conformation are existed depending on its preparation conditions and treatments [122, 123]. Here, CD analysis was conducted for analyzing the

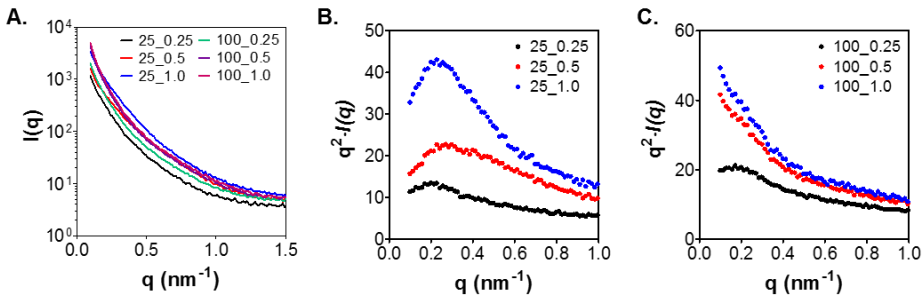


Figure 42. (A) SAXS curves and Kratky plots of SFMA hydrogels formed of different immobilized MA amount on SF and molecular weight of SF. (A) 25 kDa SF, (B) 100 kDa.

secondary structures of chemically crosslinked SF hydrogel in accordance with globular structure formation. **Figure 43** shows CD spectra of a precursor solution of SFMA before hydrogel fabrication, which were prepared with different immobilized MA amount on SF and molecular weight of SF. 25_1.0 SFMA hydrogel sample showed a typical peak at 214 nm, indicating that majority of single SFMA chain exists as a β-sheet conformation in precursor solution (**Figure 43A**). On the other hand, un-modified SF samples (25_0 and 100_0) and SFMA of 100 kDa SF (100_1.0) exhibited a characteristic peak attributed to a random coil conformation (**Figure 43A and B**). It seems that β-sheet structure might be developed with an increment of hydrophobic MA immobilized onto SF, in case of low molecular weight of SF (25 kDa) used. And during gel formation of SFMA, β-sheet aggregates may be entrapped in a hydrogel network.

Based on the results of Kratky plots (**Figure 42B**) and CD spectra (**Figure 43A**), it is speculated that globular structure formed in 25_1.0 SFMA hydrogel is consisted of β-sheet structure of SF. This structural characteristic also supports the result for the appearance of G′ plateau in the 25_1.0 SFMA hydrogel sample, as shown in **Figure 41A**. However, there was no direct evidence about an effect of immobilized hydrophobic MA moiety on β-sheet structural transition of hydrolyzed SF. Further studies are required for investigating structural formation of SFMA hydrogels, which are fabricated with hydrolyzed SF and IEM, in detail.

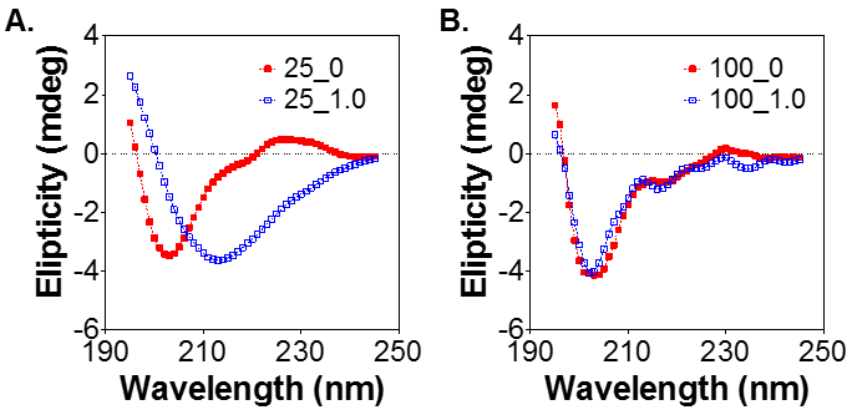


Figure 43. Circular dichroism spectra of a precursor solution of SFMA formed of different immobilized MA amount on SF and molecular weight of SF. (A) 25 kDa SF, (B) 100 kDa.

### 4.2.6. Cytotoxicity of SFMA hydrogel

SFMA hydrogels, constituted of highly MA immobilized SF (25_1.0 and 100_1.0), were incubated in serum free DMEM to evaluate cytotoxicity. During 1 day incubation in serum free DMEM, un-reacted chemicals (e.g., LAP, MA, etc.) and degraded hydrogel component may come out from the hydrogel. Relative cell viability results showed that these extracts did not exhibit a cytotoxicity for NIH-3T3 cells at any concentration condition (**Figure 44**). Moreover, as the hydrogel extracts mixed with serum free DMEM, cell proliferation was promoted up to 150% relative cell viability. Even though many *in vitro* an *in vivo* biological evaluations should be performed, SFMA hydrogel (photo-crosslinked SF hydrogel) can be used in biomedical applications because of its non-cytotoxicity.

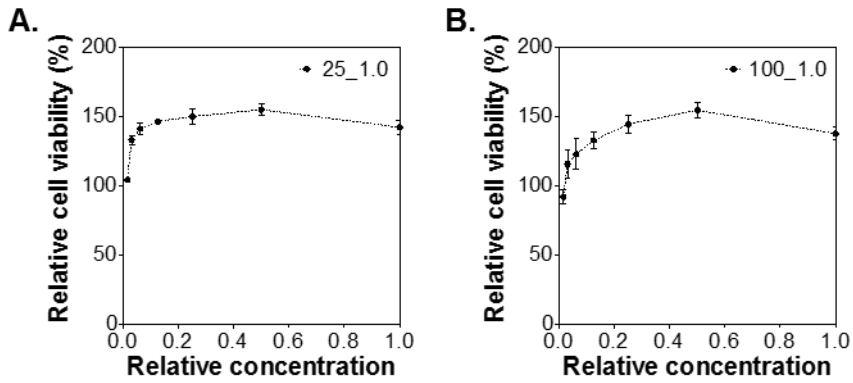


Figure 44. Relative cell viability of NIH-3T3 cells cultured on SFMA hydrogel (sample ID: 25_1.0 and 100_1.0) extracts contained DMEM; (A) 25_1.0, (B) 100_1.0 (mean ± SD, n = 3).

# V. CONCLUSIONS

New methods for fabricating physically and chemically photo-crosslinked SF hydrogel were developed via novel molecular weight control manner and the physical properties of these hydrogels were evaluated in detail. The SF hydrogels prepared from hydrolyzed SF by using heat-alkaline treatment (HAT) method exhibited a wide variety of physical and mechanical properties, dependent on the molecular weight of SF. It was found that molecular weight of SF significantly affected the gelation, swelling behavior, equilibrium shear elastic modulus, and optical property of SF hydrogel. Such an alternation in hydrogel property was mainly due to a difference in microstructure of SF hydrogel. The shorter SF chains rendered smaller base structural units in hydrogel, resulting in relatively loose network structure with a higher porosity.

Nevertheless, physically crosslinked SF hydrogel still have some drawbacks in mechanical property (brittleness) and gelation time (long time), which can be limited in the uses of this SF hydrogel. Therefore, it is necessary to introduce the chemically crosslinkable moiety into SF. It was found that lowering the molecular weight of SF enabled the direct chemical modification of SF as well as the fabrication of photo-crosslinkable SF hydrogel. In addition, photo-crosslinkable hydrolyzed silk fibroin methacrylate (SFMA) could be dissolved in PBS without using fresh SF aqueous solution, which is usually required due to the stability of SF solution. The SFMA hydrogels

exhibits excellent physical properties and high performance. It was found that both of immobilized MA amount and molecular weight of SF affected the gelation, swelling behavior, equilibrium shear elastic modulus, and degradation of SFMA hydrogel. Difference in variable properties of the hydrogels was mainly due to a characteristics of microstructure (rigidity of crosslinked network), constituted of MA groups immobilized onto SF. In particular, the SFMA hydrogel showed a rapid gel formation and an advanced physical property, such as transparency, resilience, and injectability, etc., which were not exhibited in conventional physically crosslinked SF hydrogel. It is expected that structural characteristic, high performance, and unique tailed properties of the physically as well as chemically photo-crosslinked SF hydrogel can be useful for designing advanced silk-based hydrogel material in biomedical application fields.

# VI.REFERENCES

[1] B. Kundu, N.E. Kurland, S. Bano, C. Patra, F.B. Engel, V.K. Yadavalli, S.C. Kundu, Silk proteins for biomedical applications: bioengineering perspectives, *Progress in polymer science*, 39, 251-267 (2014).

[2] B. Kundu, R. Rajkhowa, S.C. Kundu, X. Wang, Silk fibroin biomaterials for tissue regenerations, *Advanced drug delivery reviews*, 65, 457-470 (2013).

[3] E.M. Pritchard, D.L. Kaplan, Silk fibroin biomaterials for controlled release drug delivery, *Expert opinion on drug delivery*, 8, 797-811 (2011).

[4] A.B. Mathur, V. Gupta, Silk fibroin-derived nanoparticles for biomedical applications, *Nanomedicine*, 5, 807-820 (2010).

[5] C.S. Ki, Y.H. Park, H.-J. Jin, Silk protein as a fascinating biomedical polymer: structural fundamentals and applications, *Macromolecular research*, 17, 935-942 (2009).

[6] S. Kapoor, S.C. Kundu, Silk protein-based hydrogels: Promising advanced materials for biomedical applications, *Acta biomaterialia*, 31, 17-32 (2016).

[7] N. Kasoju, U. Bora, Silk fibroin in tissue engineering, *Advanced healthcare materials*, 1, 393-412 (2012).

[8] Z.-H. Li, S.-C. Ji, Y.-Z. Wang, X.-C. Shen, H. Liang, Silk fibroin-based scaffolds for tissue engineering, *Frontiers of materials science*, 7, 237-247 (2013).

[9] C. Vepari, D.L. Kaplan, Silk as a biomaterial, *Progress in polymer science*, 32, 991-1007 (2007).

[10] J.L. Drury, D.J. Mooney, Hydrogels for tissue engineering: scaffold design variables and applications, *Biomaterials*, 24, 4337-4351 (2003).

[11] L. Yu, J. Ding, Injectable hydrogels as unique biomedical materials, *Chemical society reviews*, 37, 1473-1481 (2008).

[12] S.S. Silva, T.C. Santos, M.T. Cerqueira, A.P. Marques, L.L. Reys, T.H. Silva, S.G. Caridade, J.F. Mano, R.L. Reis, The use of ionic liquids in the processing of chitosan/silk hydrogels for biomedical applications, *Green chemistry*, 14, 1463-1470 (2012).

[13] M.J. Mahoney, K.S. Anseth, Three-dimensional growth and function of neural tissue in degradable polyethylene glycol hydrogels, *Biomaterials*, 27, 2265-2274 (2006).

[14] C.M. Hassan, N.A. Peppas, Structure and applications of poly (vinyl alcohol) hydrogels produced by conventional crosslinking or by freezing/thawing methods, biopolymers· PVA hydrogels, anionic polymerisation nanocomposites, *Springer*, 37-65 (2000).

[15] I.C. Um, H. Kweon, Y.H. Park, S. Hudson, Structural characteristics and properties of the regenerated silk fibroin prepared from formic acid, *International journal of biological macromolecules*, 29, 91-97 (2001).

[16] Z.H. Ayub, M. Arai, K. Hirabayashi, Mechanism of the gelation of fibroin solution, *Bioscience, biotechnology, and biochemistry*, 57, 1910-1912 (1993).

[17] A. Matsumoto, J. Chen, A.L. Collette, U.-J. Kim, G.H. Altman, P. Cebe, D.L. Kaplan, Mechanisms of silk fibroin sol-gel transitions, *The journal of*

*physical chemistry B*, 110, 21630-21638 (2006).

[18] S. Nagarkar, T. Nicolai, C. Chassenieux, A. Lele, Structure and gelation mechanism of silk hydrogels, *Physical chemistry chemical physics*, 12, 3834-3844 (2010).

[19] U.-J. Kim, J. Park, C. Li, H.-J. Jin, R. Valluzzi, D.L. Kaplan, Structure and properties of silk hydrogels, *Biomacromolecules*, 5, 786-792 (2004).

[20] K. Numata, T. Katashima, T. Sakai, State of water, molecular structure, and cytotoxicity of silk hydrogels, *Biomacromolecules*, 12, 2137-2144 (2011).

[21] T. Yucel, P. Cebe, D.L. Kaplan, Vortex-induced injectable silk fibroin hydrogels, *Biophysical journal*, 97, 2044-2050 (2009).

[22] X. Wang, J.A. Kluge, G.G. Leisk, D.L. Kaplan, Sonication-induced gelation of silk fibroin for cell encapsulation, *Biomaterials*, 29, 1054-1064 (2008).

[23] I. Noh, G.-W. Kim, Y.-J. Choi, M.-S. Kim, Y. Park, K.-B. Lee, I.-S. Kim, S.-J. Hwang, G. Tae, Effects of cross-linking molecular weights in a hyaluronic acid–poly (ethylene oxide) hydrogel network on its properties, *Biomedical materials*, 1, 116-123 (2006).

[24] Y. Zhang, C.-C. Chu, The effect of molecular weight of biodegradable hydrogel components on indomethacin release from dextran and poly (DL) lactic acid based hydrogels, *Journal of bioactive and compatible polymers*, 17, 65-85 (2002).

[25] R. Fukae, M. Yoshimura, T. Yamamoto, K. Nishinari, Effect of stereoregularity and molecular weight on the mechanical properties of poly

(vinyl alcohol) hydrogel, *Journal of applied polymer science*, 120, 573-578 (2011).

[26] H.Y. Zhou, X.G. Chen, M. Kong, C.S. Liu, D.S. Cha, J.F. Kennedy, Effect of molecular weight and degree of chitosan deacetylation on the preparation and characteristics of chitosan thermosensitive hydrogel as a delivery system, *Carbohydrate polymers*, 73, 265-273 (2008).

[27] H.J. Kong, D. Kaigler, K. Kim, D.J. Mooney, Controlling rigidity and degradation of alginate hydrogels via molecular weight distribution, *Biomacromolecules*, 5, 1720-1727 (2004).

[28] M. Li, M. Ogiso, N. Minoura, Enzymatic degradation behavior of porous silk fibroin sheets, *Biomaterials*, 24, 357-365 (2003).

[29] A.T. Nguyen, Q.L. Huang, Z. Yang, N. Lin, G. Xu, X.Y. Liu, Crystal networks in silk fibrous materials: from hierarchical structure to ultra performance, *Small*, 11, 1039-1054 (2015).

[30] M. Lee, S. Seo, J.C. Kim, A β-cyclodextrin, polyethyleneimine and silk fibroin hydrogel containing Centella asiatica extract and hydrocortisone acetate: releasing properties and in vivo efficacy for healing of pressure sores, *Clinical and experimental dermatology*, 37, 762-771 (2012).

[31] F. Ak, Z. Oztoprak, I. Karakutuk, O. Okay, Macroporous silk fibroin cryogels, *Biomacromolecules*, 14, 719-727 (2013).

[32] T. Srisawasdi, K. Petcharoen, A. Sirivat, A.M. Jamieson, Electromechanical response of silk fibroin hydrogel and conductive polycarbazole/silk fibroin hydrogel composites as actuator material, *Materials*

*science and engineering: C*, 56, 1-8 (2015).

[33] M. Parkes, C. Myant, D. Dini, P. Cann, Tribology-optimised silk protein hydrogels for articular cartilage repair, *Tribology international*, 89, 9-18 (2015).

[34] W.H. Elliott, W. Bonani, D. Maniglio, A. Motta, W. Tan, C. Migliaresi, Silk hydrogels of tunable structure and viscoelastic properties using different chronological orders of genipin and physical cross-linking, *ACS applied materials & interfaces*, 7, 12099-12108 (2015).

[35] B.P. Partlow, C.W. Hanna, J. Rnjak-Kovacina, J.E. Moreau, M.B. Applegate, K.A. Burke, B. Marelli, A.N. Mitropoulos, F.G. Omenetto, D.L. Kaplan, Highly tunable elastomeric silk biomaterials, *Advanced functional materials*, 24, 4615-4624 (2014).

[36] S. Das, F. Pati, Y.-J. Choi, G. Rijal, J.-H. Shim, S.W. Kim, A.R. Ray, D.-W. Cho, S. Ghosh, Bioprintable, cell-laden silk fibroin–gelatin hydrogel supporting multilineage differentiation of stem cells for fabrication of three-dimensional tissue constructs, *Acta biomaterialia*, 11, 233-246 (2015).

[37] M.B. Applegate, B.P. Partlow, J. Coburn, B. Marelli, C. Pirie, R. Pineda, D.L. Kaplan, F.G. Omenetto, Photocrosslinking of silk fibroin using riboflavin for ocular prostheses, *Advanced materials*, 28, 2417-2420 (2016).

[38] N.E. Kurland, T. Dey, C. Wang, S.C. Kundu, V.K. Yadavalli, Silk protein lithography as a route to fabricate sericin microarchitectures, *Advanced materials*, 26, 4431-4437 (2014).

[39] J.G. Hardy, L.M. Römer, T.R. Scheibel, Polymeric materials based on

silk proteins, *Polymer*, 49, 4309-4327 (2008).

[40] S. Inoue, K. Tanaka, F. Arisaka, S. Kimura, K. Ohtomo, S. Mizuno, Silk fibroin of Bombyx mori is secreted, assembling a high molecular mass elementary unit consisting of H-chain, L-chain, and P25, with a 6: 6: 1 molar ratio, *Journal of biological chemistry*, 275, 40517-40528 (2000).

[41] J. Magoshi, Y. Magoshi, S. Nakamura, Mechanism of fiber formation of silkworm, ACS symposium series (USA), (1994).

[42] M. Andersson, J. Johansson, A. Rising, Silk spinning in silkworms and spiders, *International journal of molecular sciences*, 17, 1290-1303 (2016).

[43] G.H. Altman, F. Diaz, C. Jakuba, T. Calabro, R.L. Horan, J. Chen, H. Lu, J. Richmond, D.L. Kaplan, Silk-based biomaterials, *Biomaterials*, 24, 401-416 (2003).

[44] Y. Cao, B. Wang, Biodegradation of silk biomaterials, *International journal of molecular sciences*, 10, 1514-1524 (2009).

[45] H.J. Cho, C.S. Ki, H. Oh, K.H. Lee, I.C. Um, Molecular weight distribution and solution properties of silk fibroins with different dissolution conditions, *International journal of biological macromolecules*, 51, 336-341 (2012).

[46] J.-P. Chen, S.-H. Chen, G.-J. Lai, Preparation and characterization of biomimetic silk fibroin/chitosan composite nanofibers by electrospinning for osteoblasts culture, *Nanoscale research letters*, 7, 170-180 (2012).

[47] S. Zarkoob, R. Eby, D.H. Reneker, S.D. Hudson, D. Ertley, W.W. Adams, Structure and morphology of electrospun silk nanofibers, *Polymer*, 45, 3973-

3977 (2004).

[48] D.N. Rockwood, R.C. Preda, T. Yücel, X. Wang, M.L. Lovett, D.L. Kaplan, Materials fabrication from Bombyx mori silk fibroin, *Nature protocols*, 6, 1612-1631 (2011).

[49] R. Nazarov, H.-J. Jin, D.L. Kaplan, Porous 3-D scaffolds from regenerated silk fibroin, *Biomacromolecules*, 5, 718-726 (2004).

[50] C. Correia, S. Bhumiratana, L.-P. Yan, A.L. Oliveira, J.M. Gimble, D. Rockwood, D.L. Kaplan, R.A. Sousa, R.L. Reis, G. Vunjak-Novakovic, Development of silk-based scaffolds for tissue engineering of bone from human adipose-derived stem cells, *Acta biomaterialia*, 8, 2483-2492 (2012).

[51] U.-J. Kim, J. Park, H.J. Kim, M. Wada, D.L. Kaplan, Three-dimensional aqueous-derived biomaterial scaffolds from silk fibroin, *Biomaterials*, 26, 2775-2785 (2005).

[52] I.C. Um, H. Kweon, K.G. Lee, D.W. Ihm, J.-H. Lee, Y.H. Park, Wet spinning of silk polymer: I. effect of coagulation conditions on the morphological feature of filament, *International journal of biological macromolecules*, 34, 89-105 (2004).

[53] D.M. Phillips, L.F. Drummy, R.R. Naik, C. Hugh, D.M. Fox, P.C. Trulove, R.A. Mantz, Regenerated silk fiber wet spinning from an ionic liquid solution, *Journal of materials chemistry*, 15, 4206-4208 (2005).

[54] B.-M. Min, G. Lee, S.H. Kim, Y.S. Nam, T.S. Lee, W.H. Park, Electrospinning of silk fibroin nanofibers and its effect on the adhesion and spreading of normal human keratinocytes and fibroblasts in vitro,

*Biomaterials*, 25, 1289-1297 (2004).

[55] C.S. Ki, J.W. Kim, J.H. Hyun, K.H. Lee, M. Hattori, D.K. Rah, Y.H. Park, Electrospun three-dimensional silk fibroin nanofibrous scaffold, *Journal of applied polymer science*, 106, 3922-3928 (2007).

[56] S.Y. Park, C.S. Ki, Y.H. Park, H.M. Jung, K.M. Woo, H.J. Kim, Electrospun silk fibroin scaffolds with macropores for bone regeneration: an in vitro and in vivo study, *Tissue engineering part A*, 16, 1271-1279 (2010).

[57] H. Kweon, I. Um, Y. Park, Thermal behavior of regenerated Antheraea pernyi silk fibroin film treated with aqueous methanol, *Polymer*, 41, 7361-7367 (2000).

[58] H. Kweon, H.C. Ha, I.C. Um, Y.H. Park, Physical properties of silk fibroin/chitosan blend films, *Journal of applied polymer science*, 80, 928-934 (2001).

[59] C. Jiang, X. Wang, R. Gunawidjaja, Y.H. Lin, M.K. Gupta, D.L. Kaplan, R.R. Naik, V.V. Tsukruk, Mechanical properties of robust ultrathin silk fibroin films, *Advanced functional materials*, 17, 2229-2237 (2007).

[60] Y. Baimark, P. Srihanam, Y. Srisuwan, P. Phinyocheep, Preparation of porous silk fibroin microparticles by a water-in-oil emulsification-diffusion method, *Journal of applied polymer science*, 118, 1127-1133 (2010).

[61] M.K. Kim, K.H. Lee, Fabrication of porous silk fibroin microparticles by electrohydrodynamic spraying, *Polymer Korea*, 38, 98-102 (2014).

[62] M.K. Kim, J.Y. Lee, H. Oh, D.W. Song, H.W. Kwak, H. Yun, I.C. Um, Y.H. Park, K.H. Lee, Effect of shear viscosity on the preparation of sphere-

like silk fibroin microparticles by electrospraying, *International journal of biological macromolecules*, 79, 988-995 (2015).

[63] M.W. Tibbitt, K.S. Anseth, Hydrogels as extracellular matrix mimics for 3D cell culture, *Biotechnology and bioengineering*, 103, 655-663 (2009).

[64] H.-J. Jin, D.L. Kaplan, Mechanism of silk processing in insects and spiders, *Nature*, 424, 1057-1061 (2003).

[65] L. Ma, W. He, A. Huang, L. Li, Q. Wei, Z. Huang, Mechanism of conformational transition of silk fibroin in alcohol-water mixtures, *Chinese journal of chemistry*, 29, 877-882 (2011).

[66] A.N. Mitropoulos, B. Marelli, C.E. Ghezzi, M.B. Applegate, B.P. Partlow, D.L. Kaplan, F.G. Omenetto, Transparent, nanostructured silk fibroin hydrogels with tunable mechanical properties, *ACS biomaterials science & engineering*, 1, 964-970 (2015).

[67] M.L. Floren, S. Spilimbergo, A. Motta, C. Migliaresi, Carbon dioxide induced silk protein gelation for biomedical applications, *Biomacromolecules*, 13, 2060-2072 (2012).

[68] R.R. Mallepally, M.A. Marin, M.A. McHugh, CO 2-assisted synthesis of silk fibroin hydrogels and aerogels, *Acta biomaterialia*, 10, 4419-4424 (2014).

[69] Y.Y. Wang, Y.D. Cheng, Y. Liu, H.J. Zhao, M.Z. Li, The effect of ultrasonication on the gelation velocity and structure of silk fibroin, *Trans tech publications*, 175, 143-148 (2011).

[70] G.G. Leisk, T.J. Lo, T. Yucel, Q. Lu, D.L. Kaplan, Electrogelation for protein adhesives, *Advanced materials*, 22, 711-715 (2010).

[71] Q. Lu, Y. Huang, M. Li, B. Zuo, S. Lu, J. Wang, H. Zhu, D.L. Kaplan, Silk fibroin electrogelation mechanisms, *Acta biomaterialia*, 7, 2394-2400 (2011).

[72] G.D. Kang, J.H. Nahm, J.S. Park, J.Y. Moon, C.S. Cho, J.H. Yeo, Effects of poloxamer on the gelation of silk fibroin, *Macromolecular rapid communications*, 21, 788-791 (2000).

[73] F. Zhang, J. Li, T. Zhu, S. Zhang, S.C. Kundu, S. Lu, Potential of biocompatible regenerated silk fibroin/sodium N-lauroyl sarcosinate hydrogels, *Journal of biomaterials science, polymer edition*, 26, 780-795 (2015).

[74] T. Hanawa, A. Watanabe, T. Tsuchiya, R. Ikoma, M. Hidaka, M. Sugihara, New oral dosage form for elderly patients: preparation and characterization of silk fibroin gel, *Chemical and pharmaceutical bulletin*, 43, 284-288 (1995).

[75] X. Wu, J. Hou, M. Li, J. Wang, D.L. Kaplan, S. Lu, Sodium dodecyl sulfate-induced rapid gelation of silk fibroin, *Acta biomaterialia*, 8, 2185-2192 (2012).

[76] Z. Li, Z. Zheng, Y. Yang, G. Fang, J. Yao, Z. Shao, X. Chen, Robust protein hydrogels from silkworm silk, *ACS sustainable chemistry & engineering*, 4, 1500-1506 (2016).

[77] A.R. Murphy, D.L. Kaplan, Biomedical applications of chemically-modified silk fibroin, *Journal of materials chemistry*, 19, 6443-6450 (2009).

[78] S. Min, T. Nakamura, A. Teramoto, K. Abe, Preparation and characterization of crosslinked porous silk fibroin gel, *Sen'i gakkaishi*, 54, 85-

92 (1998).

[79] G.D. Kang, K.H. Lee, C.S. Ki, Y.H. Park, Crosslinking reaction of phenolic side chains in silk fibroin by tyrosinase, *Fibers and polymers*, 5, 234-238 (2004).

[80] J.L. Whittaker, N.R. Choudhury, N.K. Dutta, A. Zannettino, Facile and rapid ruthenium mediated photo-crosslinking of Bombyx mori silk fibroin, *Journal of materials chemistry B*, 2, 6259-6270 (2014).

[81] M. Fini, A. Motta, P. Torricelli, G. Giavaresi, N.N. Aldini, M. Tschon, R. Giardino, C. Migliaresi, The healing of confined critical size cancellous defects in the presence of silk fibroin hydrogel, *Biomaterials*, 26, 3527-3536 (2005).

[82] P.H.G. Chao, S. Yodmuang, X. Wang, L. Sun, D.L. Kaplan, G. Vunjak-Novakovic, Silk hydrogel for cartilage tissue engineering, *Journal of biomedical materials research part B: applied biomaterials*, 95, 84-90 (2010).

[83] W. Zhang, X. Wang, S. Wang, J. Zhao, L. Xu, C. Zhu, D. Zeng, J. Chen, Z. Zhang, D.L. Kaplan, The use of injectable sonication-induced silk hydrogel for VEGF 165 and BMP-2 delivery for elevation of the maxillary sinus floor, *Biomaterials*, 32, 9415-9424 (2011).

[84] Y. Jin, B. Kundu, Y. Cai, S.C. Kundu, J. Yao, Bio-inspired mineralization of hydroxyapatite in 3D silk fibroin hydrogel for bone tissue engineering, *Colloids and surfaces B: biointerfaces*, 134, 339-345 (2015).

[85] H.H. Kim, J.B. Park, M.J. Kang, Y.H. Park, Surface-modified silk hydrogel containing hydroxyapatite nanoparticle with hyaluronic acid–

dopamine conjugate, *International journal of biological macromolecules*, 70, 516-522 (2014).

[86] M. Ribeiro, M.A. de Moraes, M.M. Beppu, M.P. Garcia, M.H. Fernandes, F.J. Monteiro, M.P. Ferraz, Development of silk fibroin/nanohydroxyapatite composite hydrogels for bone tissue engineering, *European polymer journal*, 67, 66-77 (2015).

[87] N.E. Davis, L.N. Beenken-Rothkopf, A. Mirsoian, N. Kojic, D.L. Kaplan, A.E. Barron, M.J. Fontaine, Enhanced function of pancreatic islets co-encapsulated with ECM proteins and mesenchymal stromal cells in a silk hydrogel, *Biomaterials*, 33, 6691-6697 (2012).

[88] W. Sun, T. Incitti, C. Migliaresi, A. Quattrone, S. Casarosa, A. Motta, Viability and neuronal differentiation of neural stem cells encapsulated in silk fibroin hydrogel functionalized with an IKVAV peptide, *Journal of tissue engineering and regenerative medicine*, online published (2015).

[89] Z. Gong, Y. Yang, Q. Ren, X. Chen, Z. Shao, Injectable thixotropic hydrogel comprising regenerated silk fibroin and hydroxypropylcellulose, *Soft matter*, 8, 2875-2883 (2012).

[90] K. Ziv, H. Nuhn, Y. Ben-Haim, L.S. Sasportas, P.J. Kempen, T.P. Niedringhaus, M. Hrynyk, R. Sinclair, A.E. Barron, S.S. Gambhir, A tunable silk–alginate hydrogel scaffold for stem cell culture and transplantation, *Biomaterials*, 35, 3736-3743 (2014).

[91] J.-Y. Fang, J.-P. Chen, Y.-L. Leu, H.-Y. Wang, Characterization and evaluation of silk protein hydrogels for drug delivery, *Chemical and*

*pharmaceutical bulletin*, 54, 156-162 (2006).

[92] N. Guziewicz, A. Best, B. Perez-Ramirez, D.L. Kaplan, Lyophilized silk fibroin hydrogels for the sustained local delivery of therapeutic monoclonal antibodies, *Biomaterials*, 32, 2642-2650 (2011).

[93] M.A. de Moraes, A. Mahl, C. Regina, M. Ferreira Silva, M.M. Beppu, Formation of silk fibroin hydrogel and evaluation of its drug release profile, *Journal of applied polymer science*, 132, 41802-41807 (2015).

[94] F.P. Seib, E.M. Pritchard, D.L. Kaplan, Self-assembling doxorubicin silk hydrogels for the focal treatment of primary breast cancer, *Advanced functional materials*, 23, 58-65 (2013).

[95] B.B. Mandal, S. Kapoor, S.C. Kundu, Silk fibroin/polyacrylamide semi-interpenetrating network hydrogels for controlled drug release, *Biomaterials*, 30, 2826-2836 (2009).

[96] J. Kundu, L.A. Poole-Warren, P. Martens, S.C. Kundu, Silk fibroin/poly (vinyl alcohol) photocrosslinked hydrogels for delivery of macromolecular drugs, *Acta biomaterialia*, 8, 1720-1729 (2012).

[97] T. Zhong, Z. Jiang, P. Wang, S. Bie, F. Zhang, B. Zuo, Silk fibroin/copolymer composite hydrogels for the controlled and sustained release of hydrophobic/hydrophilic drugs, *International journal of pharmaceutics*, 494, 264-270 (2015).

[98] N. Kojic, E.M. Pritchard, H. Tao, M.A. Brenckle, J.P. Mondia, B. Panilaitis, F. Omenetto, D.L. Kaplan, Focal infection treatment using laser-mediated heating of injectable silk hydrogels with gold nanoparticles,

*Advanced functional materials*, 22, 3793-3798 (2012).

[99] M.L. Lovett, X. Wang, T. Yucel, L. York, M. Keirstead, L. Haggerty, D.L. Kaplan, Silk hydrogels for sustained ocular delivery of anti-vascular endothelial growth factor (anti-VEGF) therapeutics, *European journal of pharmaceutics and biopharmaceutics*, 95, 271-278 (2015).

[100] W.T. Brinkman, K. Nagapudi, B.S. Thomas, E.L. Chaikof, Photo-cross-linking of type I collagen gels in the presence of smooth muscle cells: mechanical properties, cell viability, and function, *Biomacromolecules*, 4, 890-895 (2003).

[101] H. Shin, B.D. Olsen, A. Khademhosseini, The mechanical properties and cytotoxicity of cell-laden double-network hydrogels based on photocrosslinkable gelatin and gellan gum biomacromolecules, *Biomaterials*, 33, 3143-3152 (2012).

[102] H. Zhang, L. Deng, M. Yang, S. Min, L. Yang, L. Zhu, Enhancing effect of glycerol on the tensile properties of Bombyx mori cocoon sericin films, *International journal of molecular sciences*, 12, 3170-3181 (2011).

[103] Z. Gong, L. Huang, Y. Yang, X. Chen, Z. Shao, Two distinct β-sheet fibrils from silk protein, *Chemical communications*, 7506-7508 (2009).

[104] K.E. Marshall, L.C. Serpell, Structural integrity of β-sheet assembly, *Biochemical society transactions*, 37, 671-676 (2009).

[105] M.R. Krebs, E.H. Bromley, A.M. Donald, The binding of thioflavin-T to amyloid fibrils: localisation and implications, *Journal of structural biology*, 149, 30-37 (2005).

[106] G. Freddi, M. Tsukada, S. Beretta, Structure and physical properties of silk fibroin/polyacrylamide blend films, *Journal of applied polymer science*, 71, 1563-1571 (1999).

[107] I.C. Um, C.S. Ki, H. Kweon, K.G. Lee, D.W. Ihm, Y.H. Park, Wet spinning of silk polymer: II. effect of drawing on the structural characteristics and properties of filament, *International journal of biological macromolecules*, 34, 107-119 (2004).

[108] K.H. Lee, D.H. Baek, C.S. Ki, Y.H. Park, Preparation and characterization of wet spun silk fibroin/poly (vinyl alcohol) blend filaments, *International journal of biological macromolecules*, 41, 168-172 (2007).

[109] L. Yu, Z. Zhang, J. Ding, In vitro degradation and protein release of transparent and opaque physical hydrogels of block copolymers at body temperature, *Macromolecular research*, 20, 234-243 (2012).

[110] L. Wang, G. Shan, P. Pan, A strong and tough interpenetrating network hydrogel with ultrahigh compression resistance, *Soft matter*, 10, 3850-3856 (2014).

[111] L. Zhao, L. Li, G.-Q. Liu, X.-X. Liu, B. Li, Effect of frozen storage on molecular weight, size distribution and conformation of gluten by SAXS and SEC-MALLS, *Molecules*, 17, 7169-7182 (2012).

[112] K.S. Jin, D.Y. Kim, Y. Rho, V.B. Le, E. Kwon, K.K. Kim, M. Ree, Solution structures of RseA and its complex with RseB, *Journal of synchrotron radiation*, 15, 219-222 (2008).

[113] R.G. Wells, The role of matrix stiffness in regulating cell behavior,

*Hepatology*, 47, 1394-1400 (2008).

[114] R.G. Breuls, T.U. Jiya, T.H. Smit, Scaffold stiffness influences cell behavior: opportunities for skeletal tissue engineering, *The open orthopaedics journal*, 2, 103-109 (2008).

[115] S. Lin, J. Shen, Surface modification of silk fibroin films with zwitterionic phosphobetaine to improve the hemocompatibility, *Journal of wuhan university of technology-mater. Sci. Ed.*, 25, 969-974 (2010).

[116] Y. Gotoh, M. Tsukada, N. Minoura, Chemical modification of silk fibroin with cyanuric chloride-activated poly (ethylene glycol): analyses of reaction site by proton NMR spectroscopy and conformation of the conjugates, *Bioconjugate chemistry*, 4, 554-559 (1993).

[117] T.T. Le, Y. Park, T.V. Chirila, P.J. Halley, A.K. Whittaker, The behavior of aged regenerated Bombyx mori silk fibroin solutions studied by 1 H NMR and rheology, *Biomaterials*, 29, 4268-4274 (2008).

[118] O. Lam, Y. Hervaud, B. Boutevin, Homopolymerization and copolymerization of isocyanatoethyl methacrylate, *Journal of polymer science part A: polymer chemistry*, 44, 4762-4768 (2006).

[119] S. Lin-Gibson, S. Bencherif, J.A. Cooper, S.J. Wetzel, J.M. Antonucci, B.M. Vogel, F. Horkay, N.R. Washburn, Synthesis and characterization of PEG dimethacrylates and their hydrogels, *Biomacromolecules*, 5, 1280-1287 (2004).

[120] C.Z. Zhou, F. Confalonieri, M. Jacquet, R. Perasso, Z.G. Li, J. Janin, Silk fibroin: structural implications of a remarkable amino acid sequence,

*Proteins: structure, function, and bioinformatics*, 44, 119-122 (2001).

[121] S.-W. Ha, H.S. Gracz, A.E. Tonelli, S.M. Hudson, Structural study of irregular amino acid sequences in the heavy chain of Bombyx mori silk fibroin, *Biomacromolecules*, 6, 2563-2569 (2005).

[122] S.M. Kelly, T.J. Jess, N.C. Price, How to study proteins by circular dichroism, *Biochimica et biophysica acta (BBA)-proteins and proteomics*, 1751, 119-139 (2005).

[123] H. Yokoi, T. Kinoshita, Strategy for designing self-assembling peptides to prepare transparent nanofiber hydrogel at neutral pH, *Journal of nanomaterials*, 2012, 1-9 (2012).

# 초 록

본 연구에서는 열-알칼리 처리 기법을 이용한 알칼리 분해 조절과 분해 시간을 달리하여 (10-180분) 넓은 분자량 범위(77.2-258.6 kDa)를 갖는 실크 피브로인을 얻을 수 있었고 이를 통해 다양한 물성을 갖는 실크 하이드로젤을 제조할 수 있었다. 실크 피브로인의 분자량은 실크 하이드로젤의 팽윤도, 전단계수, 투과도 등 물성에 매우 큰 영향을 주었으며 구조 분석 결과 물리적 가교로 이루어진 실크 하이드로젤의 구조를 형성하는데 있어서 분자량은 매우 중요한 역할을 하는 것으로 밝혀졌다. 하지만 이러한 분자량 조절 기법을 이용하더라도 실크 하이드로젤은 여전히 잘 부서지는 열악한 역학적 성질을 나타내며 젤을 형성하는데 매우 긴 시간이 걸리는 단점을 보였다. 이러한 한계점은 화학적 광가교반응을 이용하여 실크 피브로인에 공유 결합에 의한 네트워크를 형성함으로써 극복할 수 있었다. 실크 피브로인의 용액 안정성을 향상시키기 위해 실크 피브로인의 분자량을 낮춤으로써 실크 피브로인에 직접적인 화학 개질반응이 가능하도록 메타크릴레이트가 도입된 광가교 가능한 실크 하이드로젤을 제조하였다. 실크에 고정화된 메타크릴레이트 양과 실크 분자량이 하이드로젤의 젤 특성에 미치는 영향을 살펴보았으며, 화학적 가교로 이루어진 실크 메타크릴레이트

하이드로젤의 구조 특성, 물성 및 기능성, 성능을 분석함으로써 의료용 소재로서의 잠재적인 활용가능성을 평가하였다.

---

**색인어:** 실크 피브로인, 메타크릴레이트, 하이드로젤, 알칼리 분해, 물리적 가교, 화학적 가교, 광가교

**학번: 2011-21249**